PB89-159701

Atmospheric Propagation Issues Relevant to Optical Communications

(U.S.) National Oceanic and Atmospheric Administration, Boulder, CO

Jan 89

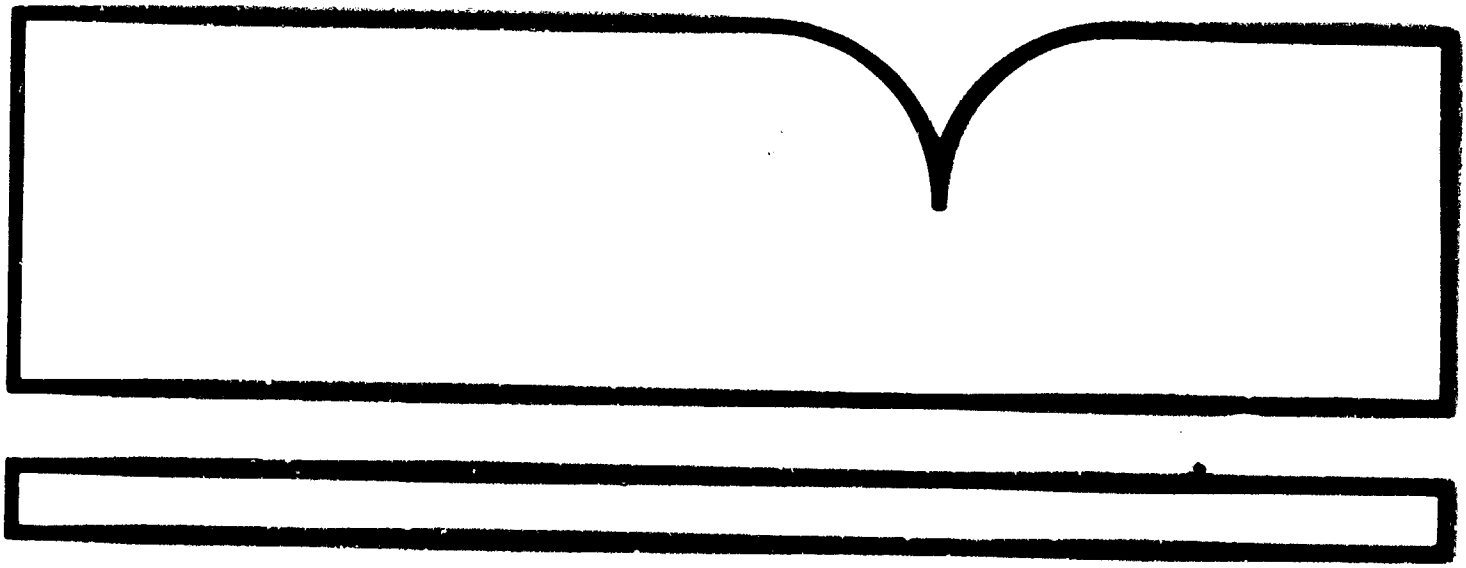

PB89-159701

NOAA Technical Memorandum ERL WPL-159

ATMOSPHERIC PROPAGATION ISSUES RELEVANT TO OPTICAL COMMUNICATIONS

James H. Churnside
Kamran Shaik

Wave Propagation Laboratory
Boulder, Colorado
January 1989

noaa NATIONAL OCEANIC AND ATMOSPHERIC ADMINISTRATION / Environmental Research Laboratories

BIBLIOGRAPHIC INFORMATION

PB89-159701

Report Nos: NOAA-TM-ERL-WPL-159

Title: Atmospheric Propagation Issues Relevant to Optical Communications.

Date: Jan 89

Authors: J. H. Churnside, and K. Shaik.

Performing Organization: National Oceanic and Atmospheric Administration, Boulder, CO. Wave Propagation Lab.**Jet Propulsion Lab., Pasadena, CA.

Type of Report and Period Covered: Technical memo.,

Supplementary Notes: Prepared in cooperation with Jet Propulsion Lab., Pasadena, CA.

NTIS Field/Group Codes: 45C, 84B

Price: PC A04/MF A01

Availability: Available from the National Technical Information Service, Springfield, VA. 22161

Number of Pages: 57p

Keywords: *Spacecraft communication, *Atmospheric scattering, *Optical communication, Light transmission, Detection, Atmospheric refraction, Turbulence, Lasers, Attenuation, Fog, Haze, Wavelength, Molecular spectra, Adsorption, Irradiance, Space flight, Mathematical models, Particulates.

Abstract: Atmospheric propagation issues relevant to space-to-ground optical communications for near-earth applications are studied. Propagation effects, current optical communication activities, potential applications, and communication techniques are surveyed. It is concluded that a direct-detection space-to-ground link using redundant receiver sites and temporal encoding is likely to be employed to transmit earth-sensing satellite data to the ground some time in the future. Low-level, long-term studies of link availability, fading statistics, and turbulence climatology are recommended to support this type of application.

NOAA Technical Memorandum ERL WPL-159

ATMOSPHERIC PROPAGATION ISSUES RELEVANT TO OPTICAL COMMUNICATIONS

James H. Churnside
Wave Propagation Laboratory

Kamran Shaik
Jet Propulsion Laboratory
California Institute of Technology
Pasadena, California

Wave Propagation Laboratory
Boulder, Colorado
January 1989

UNITED STATES DEPARTMENT OF COMMERCE

C.William Verity
Secretary

NATIONAL OCEANIC AND ATMOSPHERIC ADMINISTRATION

William E. Evans
Under Secretary for Oceans and Atmosphere/Administrator

Environmental Research Laboratories

Vernon E. Derr,
Director

NOTICE

Mention of a commercial company or product does not constitute an endorsement by NOAA Environmental Research Laboratories. Use for publicity or advertising purposes of information from this publication concerning proprietary products or the tests of such products is not authorized.

This work has been sponsored by the Jet Propulsion Laboratory under the auspicies of the National Aeronautics and Space Administration (NASA) as a part of the NASA Propagation Experimenters (NAPEX) program.

For sale by the National Technical Information Service, 5285 Port Royal Road
Springfield, VA 22161

CONTENTS

Atmospheric Propagation Issues Relevant to Optical Communications

James H. Churnside
Wave Propagation Laboratory
National Oceanic and Atmospheric Administration
Boulder, Colorado 80303

Kamran Shaik
Jet Propulsion Laboratory
California Institute of Technology
Pasadena, California 91109

ABSTRACT. Atmospheric propagation issues relevant to space-to-ground optical communications for near-earth applications are studied. Propagation effects, current optical communication activities, potential applications, and communication techniques are surveyed. It is concluded that a direct-detection space-to-ground link using redundant receiver sites and temporal encoding is likely to be employed to transmit earth-sensing satellite data to the ground some time in the future. Low-level, long-term studies of link availability, fading statistics, and turbulence climatology are recommended to support this type of application.

1. INTRODUCTION

The transfer of information from space to the surface of the earth by means of light is not a new idea. For thousands of years, visual observations of the position of the sun, the moon, and the stars have been used to obtain information about the time of day and the season of the year. Similar observations were used to obtain navigational information. Other observations, especially those made with magnifying optics in the last several hundred years, have gained information about the nature of extraterrestrial bodies transmitted from those bodies to earth through the atmosphere at optical frequencies.

From this body of experience (and other more casual observations), the qualitative features of the space-to-earth optical communication channel are known. For example, we know that the atmosphere can produce a significant amount of background light that can interfere with an optical signal. During the day, scattered sunlight is so bright that stars cannot be seen. Even at night, a full moon is bright enough that only brighter stars are visible, and scattered city light can have the same effect.

We also know that clouds can produce severe fades. Under thick clouds, no stars are visible. Even sunlight is perceived as a diffuse illumination rather than a distinct

disk, which implies that the information content of the optical signal is severely reduced. Under other conditions, less severe fades can be produced. Thin clouds or heavy haze can obscure faint stars and blur the disk of the sun, but still allow transmission of most of the optical information. This type of fade, whether severe or moderate, can persist for days.

Refractive turbulence, caused by small-scale temperature fluctuations in the atmosphere, can also cause fading of an optical signal. This effect, observed as twinkling of starlight, is much faster than aerosol-induced fading The area affected by each fade is also much smaller. If the signal is averaged over a finite disk, such as the sun, moon, or a planet, the twinkling is much less than that observed from a point source, such as a star.

One property of the atmosphere that affects the quality of optical communication is not readily apparent to the unaided eye; optical radiation is directly absorbed by the atmosphere. Spectroscopic analysis of extraterrestrial sources has demonstrated that the amount of absorption depends on the wavelength of the light and on the composition of the atmosphere. For many wavelengths the amount of water vapor in the atmosphere is particularly important.

With the development of spaceflight and of the laser, the possibility of using this channel for ground-to-space and space-to-ground communications was recognized. Several potential advantages were cited. The first was the enormous bandwidth. Green light has a frequency of 600,000 GHz and even a 1% modulation bandwidth implies incredible data transfer rates. This capability was expected to become more and more attractive as the radio spectrum became more crowded and more regulated under increasing demand for telecommunication services.

Two aspects of optical communication links were especially attractive to military planners. One is the narrow beam width. A 10-cm antenna aperture produces a 10-μrad beam. Such a narrow beam is difficult to intercept and difficult to jam. The other is the immunity to conventional electromagnetic interference enjoyed by optical links.

However, the potential has not been realized. Requirements for data rates higher than those that can be provided by microwave links have not been identified. Also, spectrum crowding has not been a limiting factor. This may be due in part to the success of fiber-optic communications. Long distance telephone service, for example, is making heavy use of fiber-optic links rather than satellite-relayed radio links. Security of space-ground optical links has been overshadowed by laser reliability limitations. Early gas and ion lasers, such as HeNe, Ar_+, and CO_2, were built around low-pressure glass tubes and were not reliable enough for routine use in space. Early solid-state lasers, such as Nd:YAG and ruby, were optically pumped using flashlamps with similar

lifetime limitations. Early semiconductor diode lasers were extremely low power devices.

Each of these factors is beginning to change, and several groups are beginning to seriously consider optical communications in space. The first application will be space-to-space relay links; more conventional technology will be used to send data to the ground. In this application, the atmospheric effects can be ignored. This is a first step toward all-optical links. Another application of interest is for satellite-to-submarine communication. However, this is a very specialized application to solve a specific problem and is unlikely to lead to widespread civilian applications.

2. ATMOSPHERIC PROPAGATION EFFECTS

The atmosphere affects optical communications in four ways. (1) Molecular absorption. Because a portion of the transmitted energy is absorbed by the atmosphere, the energy available to the receiver is reduced. (2) Particulate scattering. A portion of the transmitted energy is scattered out of the field of view of the receiver, and the energy available to the receiver is also reduced by this process. If the scatterers are dense, as in thick clouds, multiple scattering can occur and the received pulses will be spread temporally in addition to being reduced in energy. (3) Refractive turbulence. The primary effect of turbulence is to produce a random modulation of the power reaching the receiver. If the transmitted beam is very narrow, it can also reduce the average power received by spreading the beam. (4) The scattering of background light into the field of view of the receiver.

2.1 Molecular Absorption

The only effect of molecular absorption on an optical communication link is to reduce the irradiance available to the receiver.[1] In particular,

$$I = I_o \exp\left[-\int_0^L \sigma_s(z)dz\right], \tag{2.1}$$

where I is the irradiance at the receiver, I_o is the irradiance that would have been observed if there were no absorption, z is the position along the path between the transmitter and the receiver, L is the path length, and $\sigma_s(z)$ is the absorption coefficient at position z. Note that the argument of the exponential in Eq. (2.1) is also known as optical depth or optical thickness.

Light is absorbed when the quantum state of a molecule is excited from one state to another that has a greater electronic, vibrational, or rotational energy. The closer the photon energy (proportional to optical frequency) is to the transition energy, the

greater the probability of absorption (absorption cross section). Each transition is characterized as an absorption line whose peak frequency, width, and total cross section must be known.

For a single, stationary molecule, the absorption cross section has the Lorentzian line shape[2]

$$g_L(w) = \frac{T_2^{-1}}{\pi} \left[(\Omega - w)^2 + \left(\frac{1}{T_2}\right)^2 \right]^{-1} \tag{2.2}$$

where w is frequency, Ω is the center frequency of the transition, and T_2 is its duration. T_2 is of the order of 10 ns for an electronic transition, but it can be several orders of magnitude greater for vibrational or rotational transitions. The width of these lines is typically of the order of 10^{-5} nm.

In the atmosphere, thermal motion of molecules leads to Doppler broadening of the line shape; the velocity distribution of the molecules leads to a distribution of effective absorption frequencies due to the Doppler shift. In addition, molecular collisions perturb the energy levels within molecules and lead to pressure broadening of the line shape. These processes produce a Gaussian line shape[2]

$$g_G(w) = \frac{2}{\Delta w} \left(\frac{ln2}{\pi} \right)^{1/2} \exp\left[-4\, ln2\, \frac{(\Omega - w)^2}{(\Delta w)^2} \right] \tag{2.3}$$

where Δw is the width of the line. In the atmosphere, the Gaussian line width is generally much larger than the underlying Lorentzian width for any transition.

Therefore, to calculate the total absorption coefficient at a particular frequency, one must calculate the line shape factor, including temperature and pressure effects, for all lines that are close enough in frequency to have an effect. This is combined with information about the total absorption cross section for each transition and the abundance of each molecular species involved to get the absorption coefficient for each transition, and the individual coefficients are added together.

There are a number of texts on spectroscopy and catalogs of line parameters. Perhaps the most complete compilation pertinent to atmospheric transmission is the high-resolution transmittance (HITRAN) program at the Air Force Geophysical Laboratory (AFGL). The original report[3] lists line parameters (center frequency, line strength, air-broadened width, lower state energy, vibrational and rotational quantum numbers, electronic state identification, and isotopic identification) for more than 100,000 lines of the major atmospheric gases (water vapor, carbon dioxide, ozone, nitrous oxide, car-

bon monoxide, methane, and oxygen) between 1 μm and 1 mm. This data base has been periodically expanded and updated over the years,[4-9] and the most recent version includes the transition probability, the Lorentzian line width, and the temperature dependence of the Gaussian line width for almost 350,000 lines of 28 gases over a spectral region from the ultraviolet to millimeter waves.

However, for typical optical communications, the source bandwidth and receiver bandwidth will be larger than the resolution bandwidth of the HITRAN calculation. A calculation with lower spectral resolution is better matched to this application and also requires fewer computer resources to make the calculations. Such a computer code has also been developed by AFGL. The LOWTRAN[11-16] codes calculate molecular absorption from 0.25–28.5 μm. They also calculate extinction due to molecular and aerosol scattering. These codes have been used extensively, and a number of comments on their use have been published.[17-24] A typical plot of LOWTRAN6 calculated space-to-ground transmission[24] is presented in Fig. 2.1. Note that this includes the effects of molecular and aerosol scattering in addition to molecular absorption.

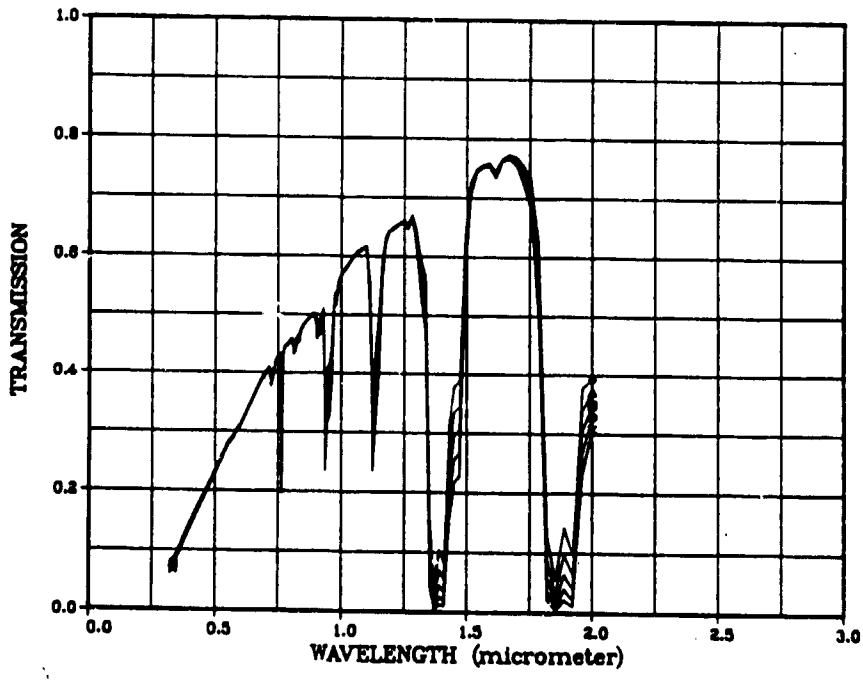

Figure 2.1 – LOWTRAN6 calculation of space-to-ground transmission as a function of wavelength. (Ref. 24)

Measurements of transmission are generally of one of three types. The first type is a laboratory measurement of the absorption of one particular atmospheric gas. Far too many such studies have been undertaken to mention here, but a few of the classical

investigations of absorption due to water vapor,[25-27] carbon dioxide,[28-30] ozone[31-33] and various trace gases[34-36] are listed in the references. Laboratory investigations of atmospheric gases are ongoing;[37-40] perhaps the largest current effort is at the Institute of Atmospheric Optics in the U.S.S.R.[41]

The second type of measurement is an absorption measurement over a long, horizontal path in the open atmosphere. One of the classic measurements was made over a 1.8-km path.[42] A typical transmittance curve from this work is presented in Fig. 2.2. Similar measurements have been made[43-49] over horizontal paths of 300 m[43] to 25 km.[44] Comparisons of horizontal path data and LOWTRAN predictions have also been made,[49-51] and the agreement is generally pretty good.

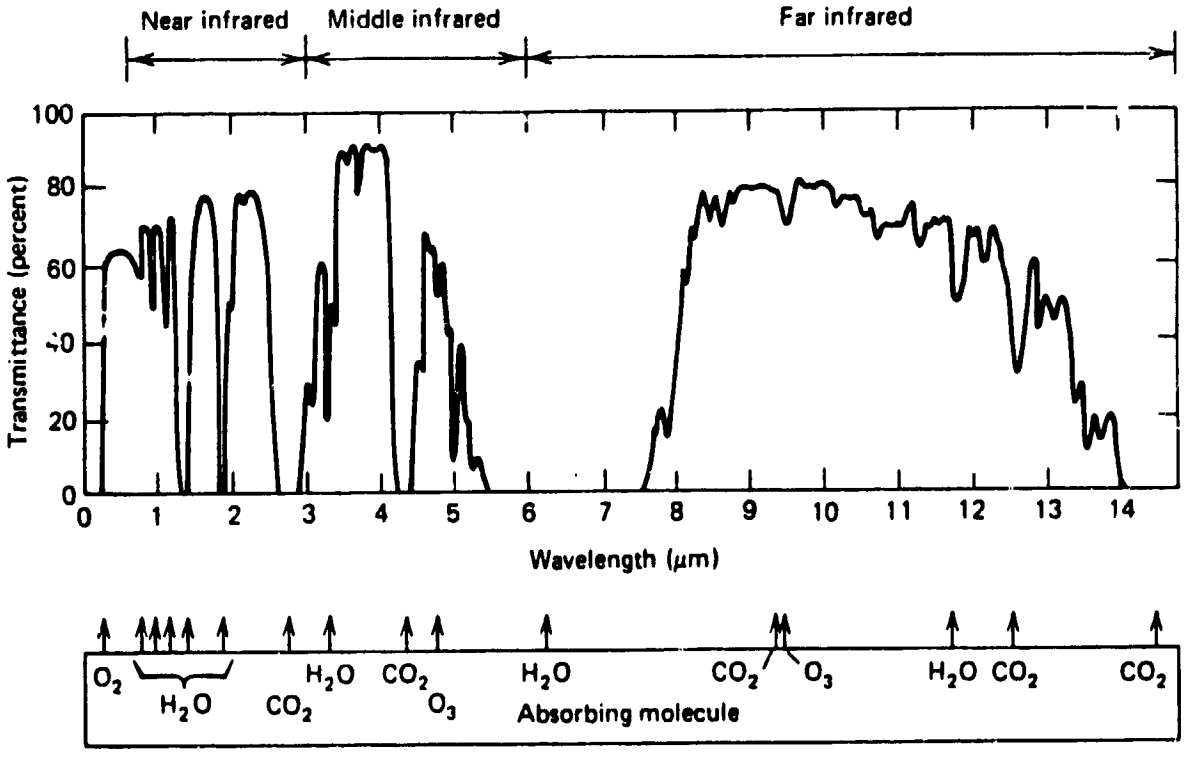

Figure 2.2 – Atmospheric transmittance for a 1.8-km horizontal path at sea level. (McCartney, Ref. 1, copyright 1976, John Wiley and Sons)

The third type of atmospheric absorption measurement uses observations of the solar spectrum. This type is probably the most closely related to space-ground communications because it is made through the entire atmosphere. A variety of measurements from different locations, different altitudes, and different spectral regions have been made.[52-66] Figure 2.3 is a typical solar spectral curve.

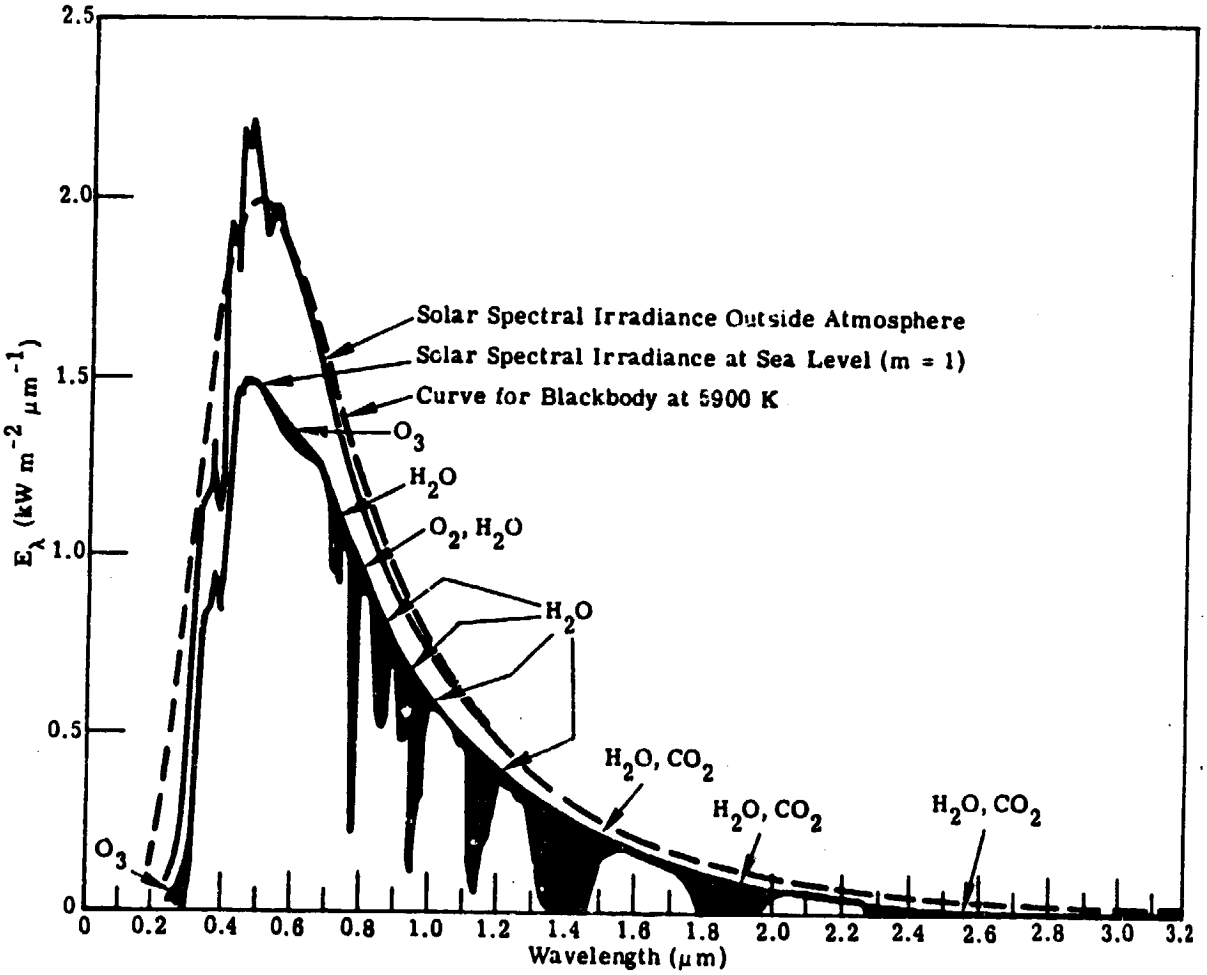

Figure 2.3 – Spectral disribution curves related to the sun. The shaded areas indicate absorption at sea level due to the atmospheric constituents shown. (Ref. 67)

2.2 Particulate Scattering

2.2.1 Scattering by air molecules

Since the air molecules are much smaller than the wavelength of light, this is the Rayleigh scattering regime.[68] In this regime, the only effect of the scattering on a communications link is extinction of the beam. As in the case of molecular absorption, we have

$$I = I_o \exp\left[-\int_0^L \sigma_R(z)dz\right] \tag{2.4}$$

where I is the irradiance at the receiver, I_o is the irradiance that would have been observed if there were no molecular scattering, and $\sigma_R(z)$ is the scattering coefficient at position z.

The scattering coefficient for a gas with refractive index of n is given by[68]

$$\sigma_R = \frac{8\pi^3(n^2-1)^2}{3N\lambda^4} \tag{2.5}$$

where N is the number of molecules of that gas per unit volume and λ is the optical wavelength. In the atmosphere, several gases (mainly nitrogen and oxygen) contribute, and the coefficients of each are added to obtain the final result. Tabulated values for various vertical paths are provided by Elterman.[69, 70] Plots of the optical thickness of the molecular scattering atmosphere for paths from space to various altitude are given in Fig. 2.4, where optical thickness is defined by

$$T_m' = \int_0^L \sigma_R(z)dz \, . \tag{2.6}$$

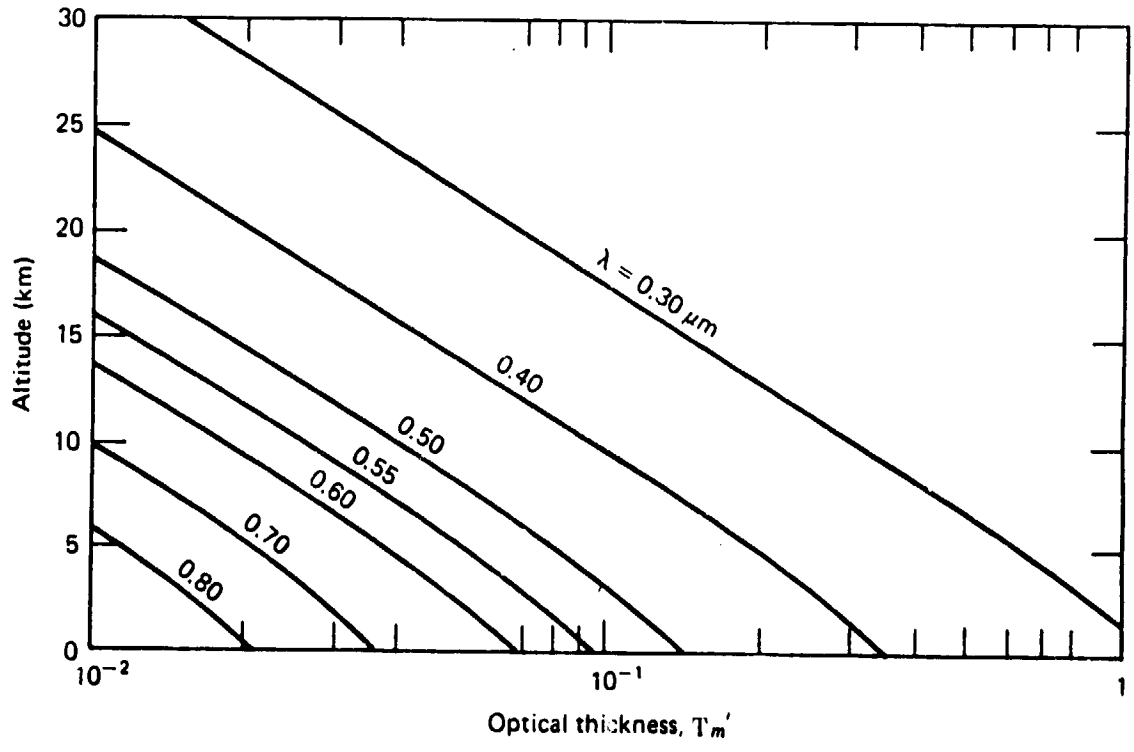

Figure 2.4 – Optical thickness of the molecular atmosphere as a function of altitude and wavelength for a vertical path, above any given altitude. (McCartney, Ref. 68, copyright 1983, John Wiley and Sons)

Molecular scattering is treated in the LOWTRAN computer codes.[11, 16]

2.2.2 Scattering by haze and thin clouds

Haze consists of solid particles in the atmosphere (dust, sea salt, volcanic ash, combustion ash, tar resin particles, etc.). It is deposited into the atmosphere by micrometeors, volcanic eruptions, industrial operations, forest fires, growing forests, and the winds. Generally, atmospheric haze particles are between 0.01 and 10 μm. Under all but the most extreme conditions encountered in the atmosphere, very few scattered photons will reach the receiver, and the effect of haze is a linear extinction so that

$$I = I_o \exp\left[-\int_0^L \sigma_M(z)dz\right] . \tag{2.7}$$

where I_o includes the effects of molecular scattering and absorption, and σ_M is the Mie scattering extinction coefficient.[71]

For our purposes, we define thin clouds as those for which Eq. (2.7) is valid. Thin cirrus and very light fogs generally fall into this category. As a rule of thumb, if the disk of the sun or moon can be seen, Eq. (2.7) will be a very close approximation.

The calculation of the Mie scattering coefficient is more difficult than that of the Rayleigh coefficient.[71] Because of the importance of Mie scattering to many areas of optics, many tables of numerically calculated values have been published. In Refs. 72 through 81, tables of the scattering coefficient and angular scattering function for various atmospheric particles are presented. The quantity of interest here, the scattering coefficient is the integral over all angles of the angular scattering function. The Mie type of scattering calculation assumes spherical particles, but although water droplets are spherical, ice crystals and many types of dust particles are not. Thus, Mie calculations may have difficulty describing the angular distribution and polarization properties of the scattered light for certain atmospheric aerosols. However, they provide a very good approximation to the total extinction coefficient.

At any height in the atmosphere, the total extinction coefficient can be found by integrating the coefficient for each type of particle over the distribution of particles. Two particle size distribution forms have been suggested. These are the exponential[82, 84] distribution

$$n(r) = ar^{\alpha} \exp(-br^{\gamma}) \tag{2.8}$$

where a, b, α, and γ are positive constants and n is the number density of particles of radius r, and the power law[85, 87]

$$n(r) = c\, r^{-v} \tag{2.9}$$

where c and v are positive constants. Measurements tend to support the power-law distribution,[85, 87-93] with an exponent v of 3 to 4.

Vertical distributions of aerosol density have been obtained using a number of techniques. One technique uses direct sampling by an airborne instrument.[91, 94-99] Another uses scattered light from searchlights[100-104] or lidar[105-111] to obtain aerosol profiles. Analysis of scattered sunlight has also been used to infer aerosol profiles.[112-119]

Long-path measurements of the attenuation coefficient due to aerosols in the atmosphere have been made by a number of authors.[42, 120-123] Typical attenuation coefficients for horizontal propagation at sea level are given in Fig. 2.5 for a variety of atmospheric conditions. Although the attenuation coefficient at sea level can be rather high, as the figure shows, it drops off quickly with altitude, as shown in Fig. 2.6. The results of vertical propagation measurements[58-60, 112-119] support this type of decrease in attenuation with altitude. Several vertical profiles of aerosol distributions, typical of different geographical regions and seasons, have been included in the LOWTRAN codes.[11-16] Therefore, these codes include a reasonable approximation of attenuation due to haze.

2.2.3 Scattering by thick clouds and fog

This type of scattering has several effects relevant to optical communications. First, the direct (unscattered) beam can be very strongly attenuated. Table 2.1 presents typical parameters for the various types of cloud and fog. The total vertical attenuation of the direct beam can be more than 1000 dB! These values are calculated from measured cloud thickness and drop distribution values and are not measured values. Indeed, measurement of a 1000 dB attenuation would be exceedingly difficult. However, laboratory[127-131] and field[132-135] tend to support these levels of attenuation. More than 100 dB has been observed for cumulus clouds.[132]

Although the direct beam is very highly attenuated, some of the original laser energy is available to the receiver in the form of multiple scattered light. This can be used for communications, but it has several disadvantages. First, the scattered light is depolarized,[68] and polarization coding of the signal cannot be used.

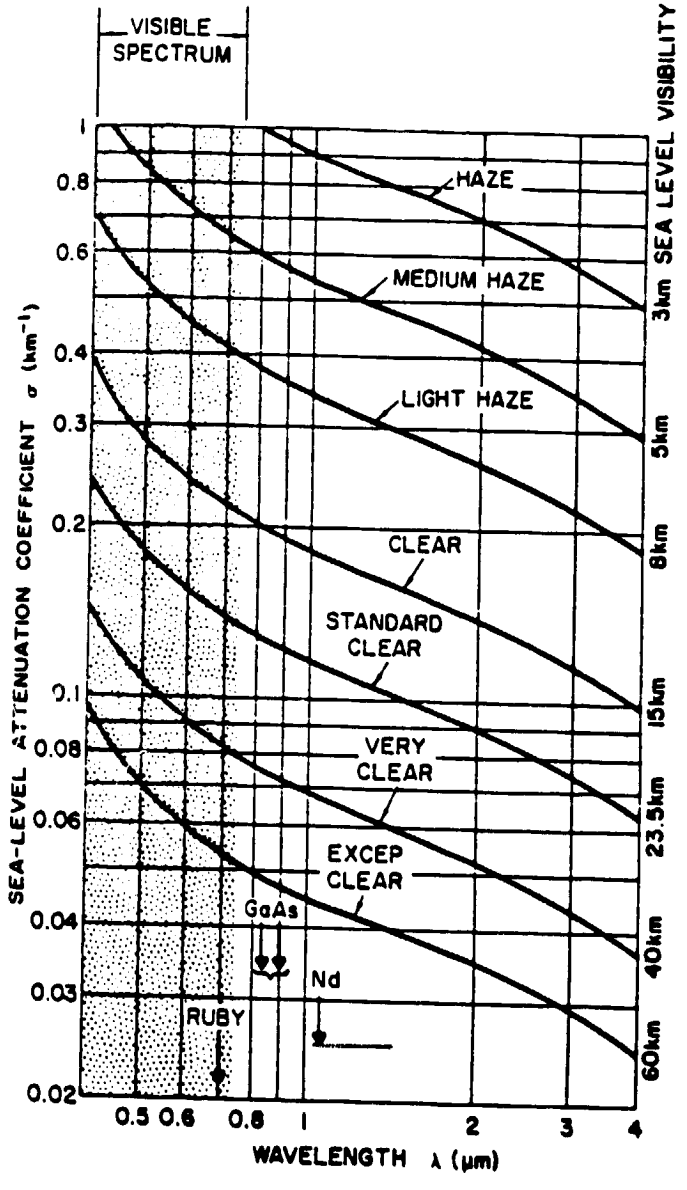

Figure 2.5 – Approximate variation of attenuation coefficients with wavelength at sea level for various atmospheric conditions (neglects absorption by water vapor and carbon dioxide). (Ref. 124)

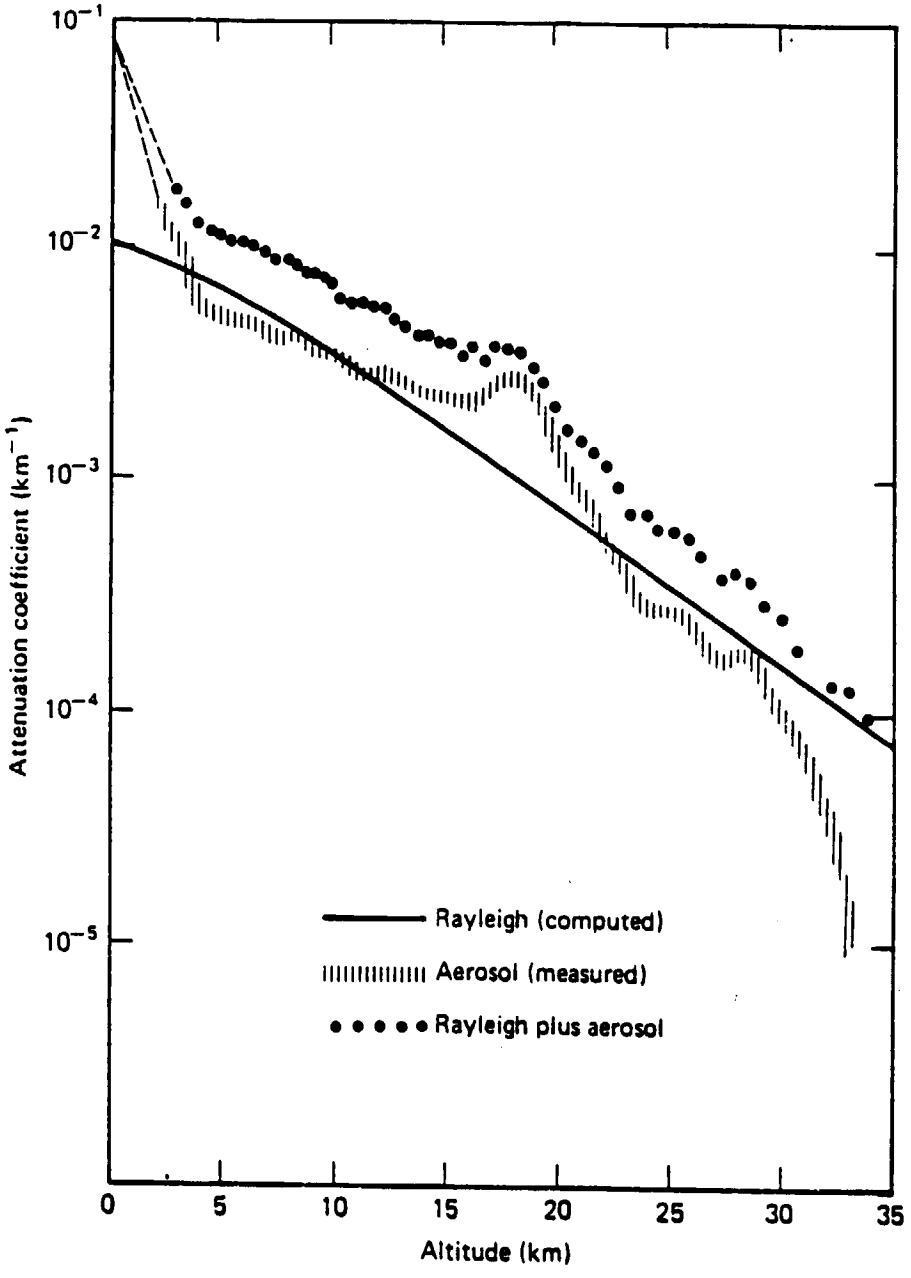

Figure 2.6 – Vertical distribution of attenuation coefficient for New Mexico aerosol (Ref. 125)

Table 2.1. Typical ranges of values for cloud parameters[126]

Cloud type	Cloud base height (km)	Cloud thickness (km)	Scattering (km^{-1})	τ in vertical direction	Scattering (dB/km)	Total vertical attenuation (dB)
Stratus	0.1–0.7	0.2–0.8	30–100	6–80	130–435	26–350
Stratocumulus	0.6–1.5	0.2–0.8	3–30	0.6–24	13–130	3–100
Nimbostratus	0.1–1.0	2–3	30–100	60–300	130–435	2660–1300
Altostratus/ Cumulus	2–6	0.2–2	10–30	2–60	43–130	9–260
Cumulus	0.5–1.0	0.5–5	10–40	5–200	43–170	22–870
Cumulonimbus	0.5–1.0	2–12	30–100	60–1200	130–435	260–5200
Cirriform (Ice)	6–10	1.0–2.5	0.3–1.4	0.3–3.5	1–6	1–15
Fog	0	0–0.15	0.1–20	0–3	0.4–87	0–13

In addition, as light diffuses through the cloud by multiple scattering, the scattered beam becomes very broad and the scattered pulse is spread in time. This implies that the receiver must have a wide field of view, which greatly increases the background noise, in order to collect enough signal power. It also implies that the data rate must be low enough to prevent intersymbol interference due to the pulse spreading. These two effects are related; the widest-angle-light reaching the receiver tends to have experienced the longest time delay. Therefore, one can allow higher data rates by restricting the field-of-view of the receiver, but the signal level is reduced dramatically. The pulse shape is generally approximated by the function[136]

$$I(t) = At \exp(-\alpha t) \tag{2.10}$$

where I is the received irradiance, t is time, and A and α are condition-dependent parameters. Pulse widths of 0.1 μs to as long as 20 μs are common in field experiments.[132, 135 - 138]

The effects of thick clouds are probably too severe to allow operation of high-data-rate optical communications. For this reason, the most important parameter for thick

clouds is the probability of occurrence, which translates into link availability. This information can be inferred for the United States and for U.S. possessions and some military bases from the Surface Airways Observations data base.[139] This data base includes hourly averages (three-hourly from 1965–1981) of ceiling height, horizontal visibility, weather type, total opaque sky cover, and total opaque sky cover. Since the records date from 1948, the statistical uncertainties in measured probabilities should be small.

2.3 Refractive Turbulence

Turbulence in the clear air produces random fluctuations in the temperature of the air. These small (0.1 to 1 K) fluctuations produce correspondingly small (0.1 to 1 ppm) fluctuations in the refractive index of the air. Although the deviation of the refractive index at any point in space and time is small, a laser beam will typically propagate through a large number of refractive index inhomogeneities, and the cumulative effect can be quite large. These inhomogeneities produce distortions of the optical phase front, which can also lead to beam wandering, beam spreading, pulse spreading, depolarization, and scintillation or intensity fluctuations. Although some of the other effects are discussed here, it is scintillation that will have the greatest effect on practical communication links.

The statistics of the refractive index fluctuations are best described by the refractive index structure function, defined by

$$D_n(\mathbf{r}) = < [n(\mathbf{r}_1) - n(\mathbf{r}_2)]^2 > \tag{2.11}$$

where n is the refractive index, $\mathbf{r}$ is the separation between the two points $\mathbf{r}_1$ and $\mathbf{r}_2$ and the angle brackets denote an ensemble average. Under typical conditions, turbulence will be nearly isotropic, and

$$\begin{aligned} D_n(r) &\approx 0 \text{ for } r < l_o \\ D_n(r) &= C_n^2 r^{2/3} \text{ for } l_o < r < L_o \\ D_n(r) &\approx C_n^2 L_o^{2/3} \text{ for } L_o < r \end{aligned} \tag{2.12}$$

where r is the magnitude of the separation, l_o is the inner scale of turbulence (typically 1 to 10 mm), L_o is the outer scale of turbulence (typically 1 to 100 m), and C_n^2 is the structure parameter of turbulence and is a measure of the strength of refractive turbulence.

A number of measurements of the vertical profile of turbulence have been made. Techniques used include in situ sensors on aircraft[140, 141] and balloons,[142, 143] acoustic sounding,[144 - 152] radar sounding,[152 - 162] and optical scintillation techniques.[163 - 175] From data like these, the following model for C_n^2 has been developed:[176]

$$C_n^2 = \{[(2.2 \times 10^{-53})h^{10}(W/27)^2]e^{-h/1000} + 10^{-16}e^{-h/1500}\} \exp[s(h,t)] , \qquad (2.13)$$

where h is the height in meters above sea level. The model is valid for 3 km < h < 24 km. The variable s is a zero-mean, homogeneous, Gaussian random variable with a covariance function given by

$$< s(h + h_1,\ t + \tau)s(h,t) > \ = A(h_1/100)e^{-\tau/5} + A(h_1/2000)e^{-\tau/80} , \qquad (2.14)$$

where

$$A(h/L) = \begin{cases} 1 - |h/L| , & |h| < L \\ 0 , & \text{otherwise} \end{cases} \qquad (2.15)$$

(The interval τ is measured in minutes.) From (2.14), it follows that $<r^2> = 2$ and $< \exp(s) > \ = e \approx 2.7$. These numbers may be substituted into (2.13), after the expected value $<C_n^2>$ is found, to determine the behavior of the mean profile. Finally, the function W in (2.13) is defined by

$$W = [(1/15\ km) \int_{5\ km}^{20\ km} v^2(h)dh]^{1/2} \qquad (2.16)$$

where v is the wind speed at height h. To extend this model down to local ground level, we should add the surface layer C_n^2 dependence, $z^{-4/3}$ during the day and $z^{-2/3}$ at night.

The depolarization by refractive turbulence has been calculated.[177, 178] Under fairly severe turbulence conditions, the depolarized power was calculated to be -160 dB of the polarized power. A measurement with -45 dB of sensitivity failed to detect any depolarization.[178] Therefore, depolarization effects can be neglected in optical communication link analyses.

The pulse spreading due to turbulence has also been calculated.[179 - 182] Typical calculated values range from 0.001 ps[179] to 1 ps,[182] corresponding to coherence

bandwidths of 10^3 GHz to 10^6 GHz. A coherence bandwidth of 77,000 GHz has been measured for the space-to-ground path using stellar source.[183] Therefore, pulse-spreading effects of the turbulent atmosphere can safely be neglected.

Distortions of the transmitted or received phase front produce a number of effects. These are most easily discussed in terms of the transverse correlation length of the field ϱ_o.[184-188] For a point source in space propagating to the ground, we have

$$\varrho_o = \left[2.91\, k^2 \sec\beta \int_0^L dh\, C_n^2(h)\right]^{-3/5} \tag{2.17}$$

where k is the optical wavenumber, β is the zenith angle of the propagation path, h is the height above the ground, and L is the altitude of the receiver. In other work, the quantity r_o has been used, where $r_o = 2.1\, \varrho_o$.[189-192] This finite correlation of the field has several effects. Increasing the diameter of an optical heterodyne antenna on the ground beyond ϱ_o will not increase its signal-to-noise ratio. The beam width of ground-to-space beam can be no narrower than the diffraction limit of a r_o-size aperture. The field-of-view of a space-to-ground-link receiver must also be at least 2.44 λ/r_o to receive all the available signal energy. For visible light, r_o is typically of the order of 10 cm,[184, 192, 193] and only heterodyne communications from space to ground will be seriously affected. Beamwidths and fields of view down to about 10 μrad can be used. Note that if angle-of-arrival fluctuations are eliminated by the tracking system, r_o can be replaced by a value about 3.4 times as large in these limits.

For propagation in the other direction,

$$\varrho_o^1 = L\left[2.91\, k^2 \sec^{8/3}\beta \int_0^L dh\, C_n^2(h) h^{5/3}\right]^{-3/5}$$

$$\approx \frac{10\ km}{L} \sec\beta\, \varrho_o \tag{2.18}$$

which implies that optical heterodyne receivers for ground-to-space links can be very large, direct detection receivers for ground-to-space links can have very narrow fields-of-view, and space-to-ground beams can be very narrow.

Therefore, for direct detection, the only significant effect of atmospheric turbulence is scintillation, or intensity fluctuations. As long as the coherence length ϱ_o is greater than the Fresnel zone size $[(\lambda h_o \sec\beta)^{1/2}$ where h_o, the effective height of the atmosphere, is about 10 km], these fluctuations will have a lognormal probability density function[194]

$$p(I) = \frac{1}{\sqrt{2\pi}\,\sigma_{\ln I} I} \exp\left[-\frac{1}{2\sigma_{\ln I}^2}\left(\ln I + 1/2\,\sigma_{\ln I}^2\right)^2\right] \tag{2.19}$$

where I is the irradiance at a point and $\sigma_{\ln I}^2$ is the variance of the logarithm of irradiance. Under conditions of high turbulence levels and/or low elevation angles, ϱ_o will not be greater than the Fresnel zone, and saturation effects become apparent in the scintillation. In the saturation regime, the point irradiance fluctuations are not lognormal.[194, 195] Many attempt to describe the probability density function of irradiance in this regime.[196 - 210] One of the more successful of these attempts is described in Refs. 207–210. It predicts that the total power collected by an aperture will be lognormally distributed as long as that aperture is larger than a Fresnel zone, and data[209] support this prediction. Since direct detection optical communication links will probably use receivers larger than a Fresnel zone, the lognormal distribution can be used for signal fading statistics.

For the uplink, ϱ_o will generally be larger than a Fresnel zone and the log-irradiance variance (spherical wave) is given by the Rytov expression[211]

$$\sigma_{\ln I}^2 = 0.56\, k^{7/6} \sec^{11/6}\beta \int_0^L dh\, C_n^2(h) h^{5/6} . \tag{2.20}$$

A typical value would probably be of the order of 0.1 for near-zenith propagation. The variance of the actual irradiance fluctuations is given by

$$\sigma_I^2 = \exp(\sigma_{\ln I}^2) - 1 \tag{2.21}$$

for the lognormal distribution.

For the downlink, the Rytov variance (plane wave), is given by[211]

$$\sigma_{\ln I}^2 = 2.24\, k^{7/6} \sec^{11/6}\beta \int_0^L dh\, C_n^2(h) h^{5/6} . \tag{2.22}$$

The actual log-irradiance variance will be below this value when this value exceeds 1 and, in fact, will never be much larger than about 1.5, owing to the effects of saturation. This saturation phenomenon has been extensively studied.[212 - 216] Figure 2.7 is a plot of log-irradiance data. The space-to-ground propagation geometry is approximated by the plane wave case in the figure. Note that these results assume a small re-

ceiver aperture. For a communications receiver, the aperture is likely to be larger than a Fresnel zone and the log-irradiance variance will be significantly reduced by the aperture averaging effect.[218-220] For unsaturated scintillations, the variance will be approximately the Rytov variance times the square of the ratio of the Fresnel zone size to the aperture diameter.

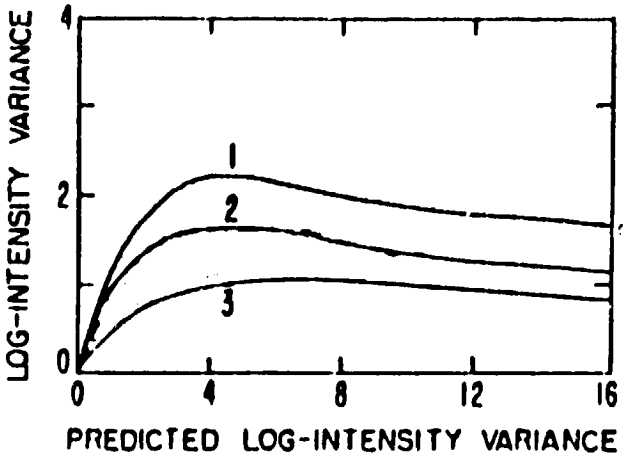

Figure 2.7 – Measured vs. predicted (Rytov) long-intensity variance for spherical wave (1), plane wave (2), and white light (3). (Refs. 211, 217)

2.4 Background Light

The effect of background light is to add noise to direct detection systems. In optical heterodyne links, the local oscillator field will be made much stronger than any background source, and background light has no effect. However, in direct detection systems, shot noise from background radiation can be a significant source of noise. The power spectral density of shot noise is given by

$$N = \frac{2\eta e^2 P}{h\nu} \tag{2.23}$$

where η is the quantum efficiency of the detector, e is the electronic charge, P is the total optical power on the detector, h is the Planck constant, and ν the angular frequency of the light. Clearly, the signal-to-noise ratio, and hence bit-error rate, will be unacceptable if the amount of background light reaching the detector is too large.

Sources of background light include direct, reflected, and scattered sunlight; thermal emission from the earth, atmosphere, moon, and planets; starlight; zodiacal light; auroral displays; direct, reflected, and scattered artificial light; bioluminescence; light-

ning; and meteor trails. However, some generalizations can be made. For the visible and near-infrared portions of the spectrum, sunlight will be the dominant background source during the day. Assuming that care is taken to ensure that the sun is never in the field of view of the receiver, the sunlight reflected from the earth will be the major contributor to the background for an uplink, and the sunlight scattered from the atmosphere will be the major contributor for a downlink. At night, moonlight, starlight, or artificial light may be the dominant source. Whichever it is, it will almost certainly be below daytime levels. Farther into the infrared, thermal emission of the earth or of the atmosphere will be the dominant background source day or night.

A general picture of the background sources important for a downlink operating during the day can be obtained from Fig. 2.8. This presents the spectral irradiance of the background light in units of microwatts of optical power per square centimeter of collector aperture area per steradian of receiver field of view per micrometer of receiver optical bandwidth for the direct sun, a sunlit cloud, clear-sky-scattered sunlight, and an atmosphere at a temperature of 300 K. Note that the direct sun is so bright that one would take care that it not be within the receiver field-of-view. Also, the presence of clouds has such a devastating effect on the operation of the link that communication through clouds is unlikely. Therefore, the sunlit cloud is unlikely to be an important background source for the uplink.

The intensity and polarization of scattered sunlight in the clear sky depend on a number of factors, including wavelength, position of the sun, direction of observation, and aerosol content of the atmosphere. Various effects and combinations of effects have been considered in the literature. References 221–238 are a representative sample of these studies; the list is by no means exhaustive. The thermal emission power also depends on a number of factors, including wavelength, atmospheric temperature, and direction of observation. A representative list of studies of this background source is provided in Refs. 221, 239-247.

For the uplink case, the earth in the vicinity of the transmitter is the background, and extensive measurements of background levels have been made by earth-imaging satellites. The Coastal Zone Color Scanner on Nimbus-7 observes the ocean at 443 nm, 520 nm, 550 nm, 670 nm, 750 nm, and 11.5 μm.[248-252] The NOAA satellites have global coverage in the visible (0.58 to 0.68 μm), near infrared (0.73 to 1.10 μm), mid-infrared (3.55 to 3.93 μm), and thermal infrared (10.5 to 11.3 μm and 11.5 to 12.5 μm) spectral regions.[253-256] Global coverage with continuous spectral coverage is provided by the Landsat series.[257-260]

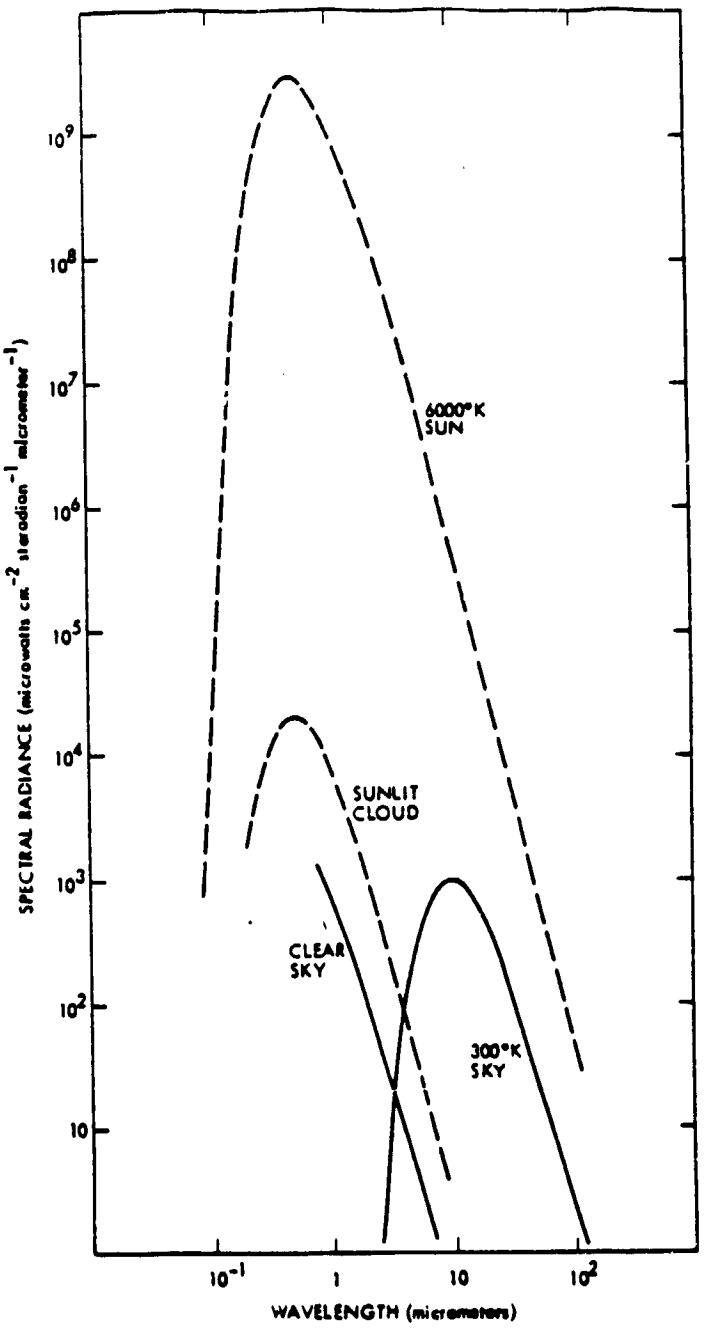

Figure 2.8 – Idealized spectral radiance of the sun (6000 K) emitting atmosphere (300 K) sunlit cloud, and sunlight scattering clear sky. (Ref. 221)

3. SURVEY OF OPTICAL COMMUNICATION ACTIVITIES

Details of the first atmospheric optical communication systems are lost in prerecorded history. Certainly, visual observation of hand motions, beacon fires, and other signaling devices was used for communication very early in the development of civilization.

In 1880, Alexander Graham Bell transmitted speech through the atmosphere using reflected sunlight.[261] This was probably the earliest system that did not rely on the human visual system, with its low frequency response, as a receiver. Shortly thereafter systems were developed that used artificial light sources instead of reflected sunlight. The major applications for these systems were military. They were used by both sides in World Wars I and II.[262] More recently, very similar systems, using light-emitting diodes or semiconductor diode lasers, have been used for communications. These systems tend to operate over very short ranges (typically of the order of 1 km or less). It is generally understood that the link will not be available during severe weather (e.g., snow).

The history of space-to-ground optical communications is much shorter. However, a number of experiments have been performed or planned (Sec. 3.2). In addition, there have been a number of theoretical studies relevant to optical communication in the atmosphere (Sec. 3.1).

3.1 Theoretical Studies

The general principles of optical communication are well known and have been the subject of books by Ross,[263] Pratt,[264] Gagliardi and Karp,[265] Kaszovsky,[266] and others. These treatments include background effects. They are also valid in the presence of molecular absorption and scattering and of scattering by haze and thin clouds. These processes have little effect beyond a reduction of the signal power reaching the detector. Fog and thick clouds do have some effect on the type of receiver one might use, but turbulence has a much larger effect and most of the theoretical studies have investigated receiver structures and performance in the presence of turbulence.

Receiver structure and performance have been evaluated for systems that use scattered light to communicate over the horizon[267] and also for the more general scatter channel that includes space-to-ground communication through clouds.[268] The major difference between the scattering channel and other channels through the atmosphere is the strong dependence, in the former, of performance on receiver field-of-view. Much of the signal energy is not collected by a receiver with a very narrow field-of-view. If the field-of-view is expanded more energy is collected and the signal-to-noise ratio improves. However, pulse spreading increases with increasing field-of-view, and this

can cause intersymbol interference and performance degration. Therefore, a tradeoff exists between signal-to-noise ratio and intersymbol interference.

The effects of intersymbol interference can be partially mitigated by signal processing within the receiver. A great deal of work has been done on this technique, called equalization, for non-optical communication channels.[269-271] Typically a tapped-delay-line filter is used on the receiver signal. A similar manipulation of received photocounts can be applied to an optical communication system that counts photons at the receiver. This problem, typical of a wide-field-of-view photon-counting receiver for a communication link through clouds, has been addressed by several authors.[272-275]

More theoretical work has been done on receiver structures and performance for propagation through refractive turbulence. The effects of turbulence on the binary communication channel for heterodyne detection were examined by Fried and Schmeltzer[276] and by Heidbreder and Mitchell.[277] From the results, it became apparent that spatial diversity techniques could be very useful in overcoming some of the deleterious effects of turbulence. Kennedy and Hoversten[278] presented the structures and error bounds for M-ary orthogonal signaling and heterodyne detection for fading on multiple, independent paths. Halme[279] extended those results to arbitrary correlation of the paths. Churnside and McIntyre[280] considered the same problem with a more realistic model for the fading statistics.

The direct detection case has also been studied. Peters and Arguello[281] considered a single channel and polarization modulation, assuming no back- ground radiation or dark current. Solimeno et al.[282] considered on-off signaling with a single detector. Background noise was considered, but in an unrealistic manner. Spatial diversity results for independent direct detection channels were presented by Hoversten et al.[279] These results were extended to include correlation of the fading by Teich and Rosenberg.[283-285] Webb and Marino[286] returned to the single-channel case and performed a more careful analysis. Churnside and McIntyre[287] developed a more sophisticated receiver structure making use of spatial diversity.

An example of the results of a receiver performance calculation for a photon-counting receiver is presented in Fig. 3.1. This is a plot of the bit-error-rate, or error probability P(E) as a function of the average number of signal photons received per channel when a 1 was sent for on-off signaling. This case assumes four independent channels and an average of one background or dark current photocount per channel. The fluctuations in the signal power at each channel are assumed to be lognormal, with a log-intensity variance of 0.25. Curve 1 represents the maximum a posteriori receiver structure.[283] Curve 2 represents an approximation to the optimum fixed maximum likelihood receiver structure.[283] Curve 3 represents an averaged threshold adap-

tive receiver structure.[287] Curve 0 represents the performance that could be obtained in the absence of turbulence; the deleterious effects of turbulence are clear. The difference that receiver structure can have on performance is also clear.

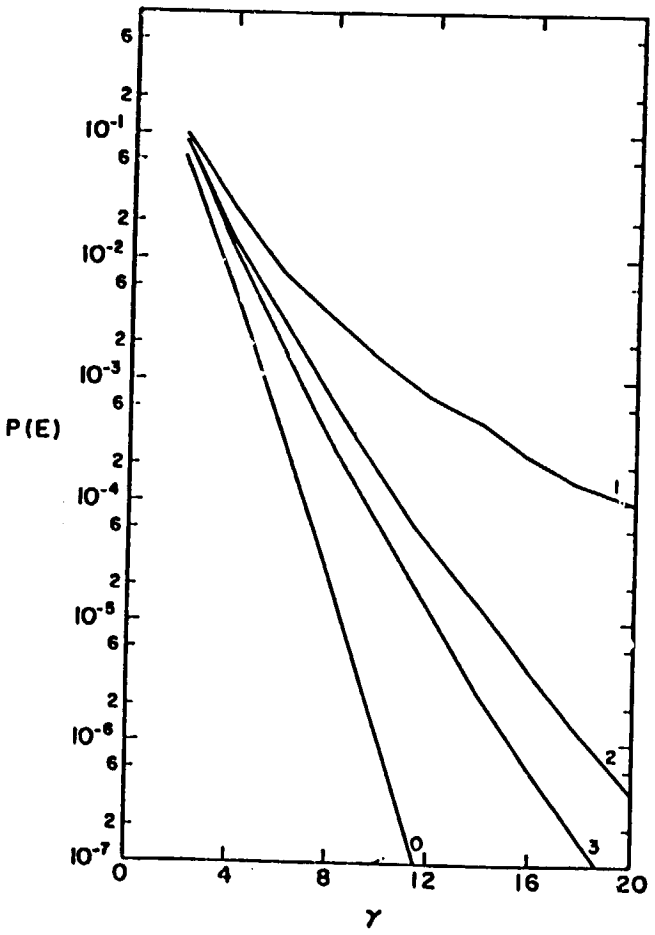

Figure 3.1 – Bit error rate P(E) as a function of the number of signal photons per bit interval for a four-channel receiver in the atmosphere. The curves represent four different receiver structures. (Ref. 287)

To our knowledge, there are no significant efforts in the theory of optical propagation through the atmosphere at the present time. The work on probability density functions in (Sec. 2.3) is very pertinent to this issue, however. The direct detection theories all assume a lognormal probability density function. If a consensus emerges on a more precise description of probability density function, it would be useful to repeat this type of receiver structure and performance study using the new density function in place of the lognormal.

3.2 Experimental Programs

To the best of our knowledge, there has been only one test of space-to- ground optical communications, and it was a failure.[262] The transmitter, designated GT-7, was developed by RCA. This device measured 7.5 x 13 x 20 cm, weighed 2.35 kg, and was designed for hand-held operation by an astronaut. It consisted of four semiconductor diode lasers with a combined peak power of 24 W into 3 mrad. It was capable of transmitting a 100 Hz acquisition tone and an 8-kHz voice channel. It was carried into earth orbit on Gemini VII in 1967. Three ground stations were each equipped with a receiving telescope and an argon ion laser beacon. The astronauts sighted the beacon at Kauai, Hawaii, on December 11, 1967, and the one at White Sands Missile Range on December 12, 1967, but no signals were received by either ground station. The beacon was visible for only a few minutes each orbit, and this was not enough time to find and lock onto the receiver station with the hand-held GT-7.

The Air Force Space Laser Communications (LASERCOM) Program started with system concept and component design in the early 1970's at the Air Force Avionics Laboratory.[288] The initial objective was to test a 1-gigabit/s space-to-ground link with a bit error rate of $<10^{-6}$ using a Nd:YAG laser transmitter. McDonnell Douglas Astronautics was chosen as the primary contractor. The program was transferred to the Air Force Space and Missile Systems Organization (now Space Division) in 1975, and a space demonstration was scheduled for a 1979 launch but was canceled because of budgetary cuts at the DoD level. A smaller, aircraft-to-ground demonstration was scheduled for 1980 at White Sands Missile Range, New Mexico.

The laser transmitter for this experiment used a K:Rb-lamp-pumped, mode-locked, frequency-doubled (to 0.53 μm wavelength) Nd:YAG laser.[288, 289] This device demonstrated 330 mW of power at 5 x 108 pulses per second, with a pulse width of 400 picoseconds. An external $TiTaO_3$ electro-optic modulator was used to produce a combination of binary pulse position and pulse polarization modulation to obtain two bits of information per pulse. The transmitter used a 20-cm-diameter telescope with a beamwidth of 5 μrad. The ground receiver used a 60-cm-diameter telescope with a field-of-view of 100 μrad. The detectors were dynamic crossed-field photomultipliers, which were followed by receiver electronics to resolve the time delay and polarization of the incoming pulses. The experiment also used a 1.06-μm laser uplink for command and control communications to the transmitter and for use as a tracking beacon by the transmitter.

Unlike the Gemini VII experiment, the LASERCOM experiment was a complete success. The system even continued to operate through some clouds, despite the fact that it was designed as a clear air system.[290] No further work on space-to-ground optical communications was done under the program. However, this work was used as a

basis for an operational space-to-space link. In the future, satellites of the Defense Satellite Program (DSP) will transfer data through a 1.2 megabit/s crosslink. This link will use a GaA/As-diode-laser-pumped Nd:YAG laser operating at 1.06 μm, pulse-position modulation, and 8-inch-diameter telescopes. The development of diode-laser-pumped Nd:YAG lasers[291-296] has produced a much more attractive laser transmitter than the original flashlamp-pumped lasers. The former are smaller, lighter, more efficient, and much more reliable than the latter.

The European Space Agency (ESA) has had a number of activities in the area of optical communications for space applications since 1977.[297] It is interested in inter-satellite links for commercial voice, television, and data transmission between two geostationary satellites and in inter-orbit links for data transmission from a low-earth-orbiting satellite to a geostationary data relay satellite.

ESA programs include research into the basic technology for CO_2 laser systems,[298-301] Nd:YAG laser systems,[302] and diode laser systems.[303-308] ESA also has a Payload and Spacecraft Demonstration and Experiment Programme (PSDE) to perform various telecommunication experiments in space. Although the final configuration of the PSDE has not been determined, one similar to that of Fig. 3.2 seems likely. It consists of two PSDE spacecraft, with optical terminals, in geostationary orbit and an optical terminal aboard a low-earth-obiting satellite, such as the French SPOT 4. Note that space-to- ground optical communications are included in this scenario. The first of the PSDE satellites is scheduled to be launched in mid-1992. The optical communication system will be a diode laser system similar to the following:[297] "The radiation of four single-mode GaAlAs laser diodes emitting around 850 nm is multiplexed to accommodate the transmission of four 120-megabit/s channels. This Wavelength Division Multiplexing technique is used to circumvent the laser output power limitation of today's available laser diodes in order to provide a return-link capacity of 500 megabit/s with moderate antenna diameters. Each laser diode is on-off keyed in the NRZ- or 4-PPM format by injection current modulation. The assumed average output power of each laser diode is 50 mW. The direct-detection receiver consists of four APD's, one for each channel. For the acquisition, a powerful laser diode array beacon sent from the GEO terminal will be used with a CCD matrix as acquisition sensor. For tracking, some 10% of the received power is directed to a monopulse tracking detector in form of a quadrant avalanche photodiode or, as recently suggested, in form of a subarray of the acquisition CCD matrix. The telescopes are of the Cassegrain type, with a gimbal as course pointing element. The diameters of the telescopes have been determined to be 35 cm on DRS and 20 cm on LEO, respectively."

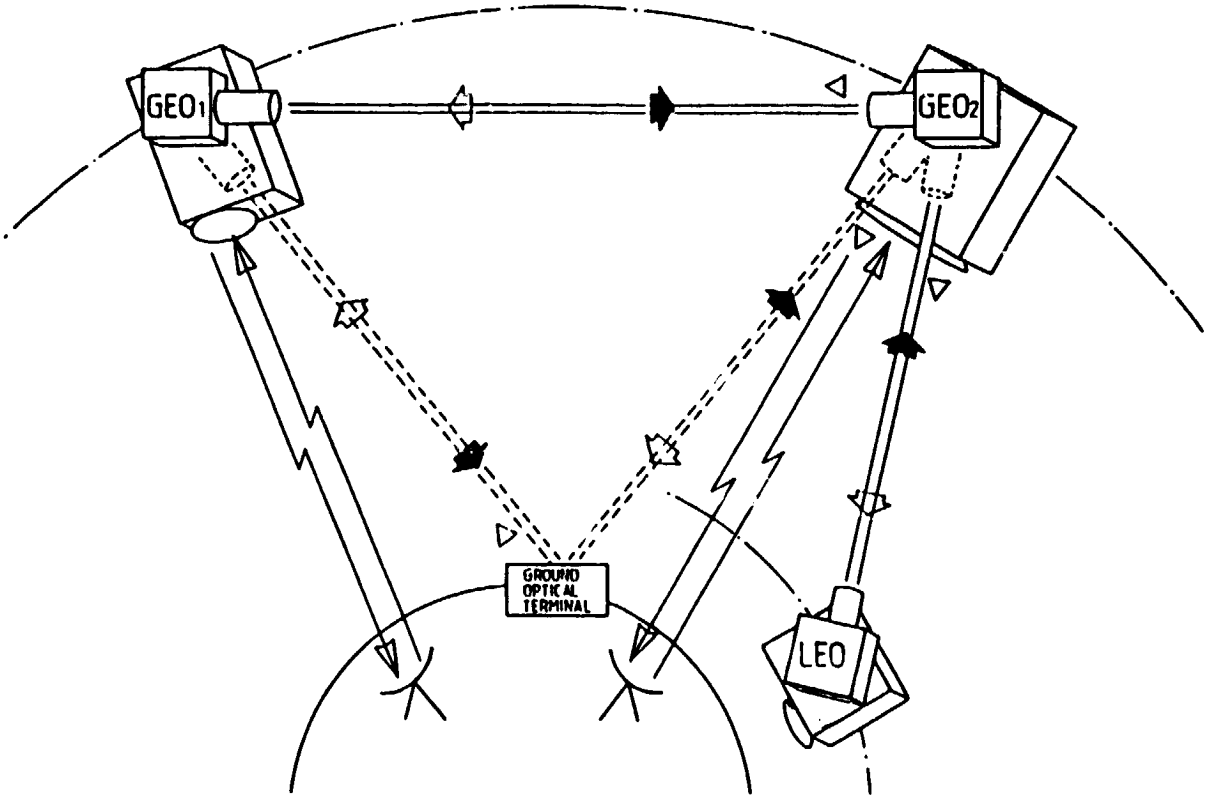

Figure. 3.2 - Possible configuration of the ESA Payload and Spacecraft Demonstration and Experiment Programme. (Ref. 297)

The ATR Optical and Radio Communications Research Laboratories of Japan are also working on optical intersatellite links.[309] These laboratories, founded in 1986, are working on technology development of diode lasers, detectors, optical integrated circuits, filters, modulation/demodulation schemes, and tracking systems. An experimental optical communication subsystem is also under consideration as one of the payloads for the Japanese Engineering Test Satellite VI scheduled for a 1992 launch. In another program, optical communications are expected to be a major experimental item aboard a large satellite that is to be assembled at a space station and put into geostationary orbit in 1996. Although the eventual application of this technology is expected to be space-to-space links, early tests are likely to be between one space terminal and a ground station, and space-to-ground communications will necessarily be investigated.

The NASA Advanced Communications Technology Satellite was also to have carried an optical communication terminal in geostationary orbit. Two different experi-

mental systems were to have used a common telescope. The first was the Air Force Laser Intersatellite Transmission Experiment, which was a coherent diode-laser transmitter operating at 220 megabits/s. The second was the NASA Direct Detection Laser Transceiver, a direct detection diode-laser transmitter and receiver package. Initial operation of these systems was to have been between geostationary orbit and the ground. A low earth-orbiting satellite was to have been launched later to allow experiments on inter-orbital links. The entire optical communication program has been canceled because of budgetary limitations.

Finally, we briefly mention the Navy's satellite-to-submarine communication program. The ocean is virtually opaque to electromagnetic waves except for extremely-low-frequency waves and blue-green light. For this reason, the Navy is interested in satellite-to-submarine communications using blue-green lasers.[310-311] Low data rates are envisioned, but a high link availability is required. Most of the work to date has been on component technology development. A laser source at the frequency of minimum oceanic absorption that is also suitable for space deployment is one area of active investigation. Another is a receiver filter that has a narrow optical passband but a wide field-of-view. However, these investigations are narrowly focused on the specific problem, and are unlikely to contribute significantly to nonmilitary applications.

4. OPTICAL COMMUNICATION APPLICATIONS

The interest in coherent optical communications follows a dominant trend in communication systems research. Communication systems with higher carrier frequencies are inherently capable of operating at higher antenna gain and modulation bandwidth. Optical frequencies ($\sim 10^{14}$ Hz) are several orders of magnitude higher than the operating carrier frequencies of the conventional radio frequency (RF) communication systems ($\sim 10^{9}$ Hz) in use today. The promise of large antenna gain and enormous modulation bandwidth, which become available at optical frequencies, provides the basic reason for the compelling interest shown by commercial, civilian, and military establishments in the development of a coherent optical communication system.

For similar modulation depths, the gain in the available bandwidth will be about 10^4-fold for optical communication systems. Also, for a given transmitter antenna size, the angular beamwidth is inversely proportional to the carrier frequency and the spatial power density at the receiver. This implies, for example, that the power density at the receiving aperture will be 10^6 times larger for an optical system with a 0.1-m antenna operating at 10^{14} Hz than for a system with 10-m antenna operating at 10^9 Hz. Optical systems with bit rates higher than 1 gigabit/s without multiplexing have been achieved; with various types of multiplexing, a 10^5 gigabit/s data rate is possible.[312]

Optical systems also promise to be smaller in size and weight and have lower power consumption, compared with RF systems having similar performance character-

istics. A decrease in the equipment size is very desirable because it will result in lower costs for putting communication satellites in space. In the case of other space missions, the advantage of size and weight will leave more room for scientific payloads and allow for more flexibility in spacecraft design.

Since optical transmitters experience relatively much lower diffractive spreading, optical communications provide excellent means for the design of secure systems with low probability of intercept and intentional or unintentional jamming. Tight laser beams also provide extensive opportunities for frequency reuse.

In short, laser communication technology has the potential to provide (1) an enormous data bandwidth for significantly improved channel performance, (2) a significant advantage in weight, size, and power consumption over RF systems, and (3) non-interacting multiple access link geometries that are amenable to extensive frequency reuse, and (4) secure systems with low probability of interception and jamming.

The commercial interest in laser communications is focused on the development of a high-quality multiplexed voice, video, and data transmission network. A network of satellites and ground stations is envisioned to move information efficiently on a global scale. However, there is strong competition from the relatively mature fiber optic communication technology. And has forced the commercial sector to lose some of its enthusiasm for the development of a global satellite communication network.

The civilian interests are based on the need to develop high throughput real-time data transfer mechanisms for remote sensing or earth resource satellites in low earth orbits. The data from low earth-orbiting satellites will, perhaps, be first transmitted to strategically placed geosynchronous satellites for subsequent transfer to appropriate ground station. Other applications include communication links to science probes in deep space for planetary and extra-planetary exploration.

5. OPTICAL COMMUNICATIONS IN THE ATMOSPHERE

The atmospheric channel for optical communication is characterized by (1) attenuation due to scattering and absorption by molecules and other particulate matter, (2) diffractive and turbulent beam spreading, (3) log-normal fading due to scintillation, (4) a coherence bandwidth of 1010 Hz or greater, (5) a long coherence time (~1 ms), and (6) a significant wavefront distortion, which, among other things, limits the power-collecting capability of a diffraction limited receiver.[182, 184, 211, 312]

Shapiro and Harney[313] developed an expression for the received power $P_R(t)$ in terms of the transmitted power $P_T(t)$ and relevant atmospheric propagation effects. Neglecting the propagation delay, we have

$$P_R(t) = P_T(t)(D_R^2/\pi\theta_T^2 Z^2)\,\epsilon\,\exp[-\tau]\,\exp[2u(t)]\,, \tag{5.1}$$

where $(D^2R/\pi\theta_T^2Z^2)$ represents free space propagation loss in terms of receiver diameter D_R, transmitter beam divergence θ_T, and path length Z; ϵ is the efficiency of the optical system, τ is the optical depth for the propagation path, and u(t) is the time-varying aperture-averaged log-amplitude fluctuation due to turbulence. $\exp[2u(t)]$ is, then, the time-varying aperture-averaged irradiance fluctuation at the receiver.

Eq. (5.1) disregards the effect of fluctuations in the angle-of-arrival at the receiver. In heterodyne systems this leads to a loss in the mixing efficiency. For direct detection schemes, the focused signal moves randomly in image plane affecting energy collection capabilities of the system at the detector. It has been shown that incorporation of tilt correction techniques into the receiver system can result in improvements as high as 8 dB.[314]

5.1 Scintillation

Scintillation causes fades and surges in received signal power. These fades may be as long as 10 ms, which is long enough to wipe out an entire message packet. The fade level F, in dB, is defined as[315]

$$F = -10\,\log[I(t)/I_m]\,, \tag{5.2}$$

where I_m is the mean and $I(t)$ is the instantaneous irradiance observed. Yura and McKinley[315] developed various results to compute the fraction of the time that a fade exceeds some given value. For the worst case scintillation, fades exceeding 3 dB occur

more than 50% of the time and fades exceeding 10 dB occur more than 10% of the time. For more reasonable values of scintillation strength, fades exceeding 10 dB occur only 1% of the time.

An obvious strategy to counter scintillation effects is to incorporate sufficient excess margin into the optical link. With this approach for an earth-space link, a margin of 20 dB will be necessary for the system to work properly 99.9% of the time under worst case scintillation. However, this costly solution to the problem can be avoided by employing temporal diversity. These methods include simple repetition of the message, coding, and interleaving. If coding is used, a careful matching of coding schemes to the channel can provide substantial improvement in performance.[316]

5.2 Opaque Clouds

Another aspect of the problem that is not readily apparent from Eq. (5.1) is the non-zero probability of opaque cloud cover. Presence of thick clouds, in general, will have a catastrophic effect on the availability of an optical communication link. Though scattered laser light is available for communication, the system has to be designed to have (1) a wide field-of-view to collect enough power, which greatly increases the background noise, and (2) a low data rate to avoid intersymbol interference due to pulse spreading. Also, polarization coding of the signal cannot be used as the scattered light is depolarized. An optical communication system designed to employ the scattered beam, then, quickly loses its advantages over the conventional systems.

An optical space network (OSN) for optical communications can be designed to avoid the clouds by employing spatial and temporal diversity. We need to identify sites for the installation of optical receiver/transmitter stations where the clouds have a low probability of occurrence. Several such sites with uncorrelated weather patterns may need be operated simultaneously to obtain desired link availability.

Cloud cover exhibits a number of cycles--nocturnal, diurnal, seasonal, and long range. A large number of databases, statistical studies, and computer models are available in the literature that describe and simulate cloud behavior. However, it is not clear how much of the information is useful or relevant to optical communications. A concrete view of the OSN is essential to help identify information that may be worthwhile for our purposes. We discuss two representative configurations of an OSN and see how spatial diversity can be employed to develop robust communication links.

5.2.1 Dispersed direct link

The network may be designed to have six to nine receiving stations roughly equidistant from each other, and placed around the globe near the equatorial region. The interstation distance would be roughly 5000 km, and the individual sites would be chosen

for their high probability of clear weather. Since the characteristic scale of a weather pattern or a climatic zone are of the order of a few hundred kilometers, the adjacent stations would lie in different climatic regions and thus have uncorrelated cloud cover statistics. The described arrangement of the receiving sites would ensure that at least three of them are able to intercept the signal at all times. It would be necessary work out joint cloud cover statistics for two or more consecutive sites for link availability. The probability of an outage for this configuration is low because (1) several stations would be monitoring the signal jointly or the spacecraft would have the ability to point to one of several stations by choosing the optimum site for cloud-free optical communication, and (2) the stations would lie in different climatic zones and hence their weather patterns are uncorrelated. Since the receiving sites are far apart, there would be no initial need to obtain high-resolution data on cloud cover. Later, to examine and validate a short list of likely sites, high-resolution site-specific data would be required. The temporal resolution of the data has to be high for short-term outage statistics to be computed accurately. For validation purposes we would need to do a cloud-free line-of-sight (CFLOS) and cloud-free arc (CFARC) analysis to compute outage probabilities for single sites as well as jointly for two or more sites.

5.2.2 Clustered direct link

For geophysical and/or geopolitical reasons, the OSN may consist of only three or four locations around the globe, chosen for their optimally cloud free skies. In this configuration, a cluster of two or more autonomous receiving stations could be built on each location. Note that this geometry also includes the case in which a single geosynchronous satellite, which accepts messages from other satellites, planes, and ground stations, is linked to a single cluster of receiving stations. Let us consider an extreme situation in which the receiving stations are only a few tens of kilometers apart from each other at each of the selected regions. For a major portion of the time the spacecraft can point to only one of these clusters, handing off the signal beam to the next cluster as it rises above the horizon.

We would need to do most of the studies listed in Sec. 5.2.1 to determine the suitability of sites for ground stations. However, spatial resolution on sky cover in this case needs to be very high (about an order of magnitude better than the distance between the ground sites). The stations would all be in the same climatic zone, and hence their weather patterns would be correlated. An ultra-high temporal resolution may be necessary to extract meaningful statistics. The outage times when all the ground stations are unable to receive would happen more often and would be of longer duration, compared with the dispersed configuration discussed in Sec. 5.2.1 for the same number of receivers on ground.

5.3 Weather Models and Simulations

Almost all data and statistics currently available on cloud cover are not readily amenable to the study of optical communications through the atmosphere. The next best thing to do is to use available weather data, which are incomplete and insufficient, as a guide to develop computer models and simulations that mimic real-time dynamic behavior of clouds. An early model for cloud cover was developed by scientists at SRI International. Work at AFGL, which is based on the SRI model, has produced considerably more sophisticated computer simulations of cloud dynamics. The computer programs developed by AFGL may be used to compute cloud-free line-of-sight (CFLOS) or cloud-free arc (CFARC) probabilities for any site. It is also possible to compute joint CFLOS and CFARC probabilities for two or more sites. These statistics, needless to say, are of great importance to the development of an OSN.

Shaik[317] proposed a simple heuristic weather model that can be used to compute link availability statistics. The model can be used to predict joint probability for the percentage time for which weather is such that the extinction loss through the atmosphere is less than some threshold for at least one of the ground stations. If $\omega_n(\tau)$ is the cumulative distribution function (CDF) giving percentage weather for n sites for which the optical depth of the atmosphere is less than or equal to τ, then the model states that

$$\omega_n(\tau) = 1 - \{q \exp[-b(\tau - \tau_o)]\}^n , \quad (\tau \geq \tau_o) , \tag{5.3}$$

where τ_o is an empirical constant representing the minimum possible optical depth of the atmosphere associated with an average clear day, b is a site-dependent parameter to model the slope of the CDF curve, and q is the probability of non-clear skies and is assumed, for simplicity, to be the same for all sites. The probability of non-clear skies, for example, in the southwestern United States is less than 0.4.[318] For a single site with $q = 0.4$, $\tau_o = 0.6$(2.6 dB extinction loss), and $b = 0.05$, the probability that the optical depth $\tau \leq 1.0$ (-4.3 dB) is $\omega_1(\tau = 1) = 0.61$. If there are three such independent and identically distributed sites, we have $\omega_3(\tau = 1) = 0.94$. In other words, if a system is designed to absorb extinction loss of 4.3 dB, a three-site receiving network will be functional 94% of the time. However, it is not very clear how the independence of weather patterns at various sites can be ensured. It is known, as noted earlier, that the scale size of weather patterns is of the order of a few hundred kilometers, and this measure may be used to find sites with uncorrelated weather. Joint observation of weather parameters for the probable sites will be necessary to make a more accurate determination.

5.4 Other Diversity Techniques

We have discussed path or site diversity in some detail in Sec. 5.3 because it appears to be one of the most important techniques for the design of robust optical communication links. We have also touched on temporal diversity to overcome short-term turbulence-induced fades. Brandinger[319] and Engelbrecht[320] suggested a number of other diversity techniques. Among them are (1) frequency diversity, (2) transmitter power diversity, and (3) transmission delay or temporary data storage diversity.

Apart from strong molecular scattering and absorption lines, the effect of the atmosphere on optical frequencies does not change much over the entire range. For example, the refractive index of the atmosphere changes by 10%, and the effect of changing humidity is quite small for all optical frequencies. It may be concluded that the use of frequency diversity cannot provide acceptable engineering gain in system design.

The use of transmitter power diversity can be a feasible solution to counter the loss through the atmosphere, especially for the uplink configuration. The power output of ground lasers may be adjusted so as to maintain a constant power level at the spacecraft receiver. However, the transmitter configurations on spacecraft at present must use maximum attainable laser power, leaving little room for the use of power diversity.

Temporary storage diversity is an attractive alternative, but only when real-time operation is not necessary.

6. CONCLUSIONS AND RECOMMENDATIONS

The general trend toward higher and higher frequencies and the potential bandwidth, weight, size, and power characteristics of optical links make the eventual application of optical communications inevitable. The first civil applications will probably be satellite crosslinks, following the example of the military. The first applications involving atmospheric propagation will probably be space-to-ground data links. The most promising link would use direct detection. Multiple receiver stations would be used to ensure a high probability of cloud-free propagation. To reduce the effects of scintillation, encoding of the signal would be employed.

Based on these conclusions, we do not recommend a large program in atmospheric near-Earth optical communications at NASA. However, we recommend that NASA begin to assemble the knowledge base that will allow evaluation of specific optical systems as the need arises. In particular, several investigations should be initiated now. The first is a study of link availability based on the probability of one of several potential receiver sites having a cloud-free line of sight to a particular section of the sky. The second is a study of the fading statistics for large direct-detection receivers in the

turbulent atmosphere. The last is an investigation into the climatology of turbulence levels that would aid in site selection. These three areas are recommended for long-term, low level-of-effort of study.

7. REFERENCES

1. E.J. McCartney, Absorption and Emission by Atmospheric Gases. (Wiley, New York, 1983), pp. 34–39.

2. R.H. Pantell and H.E. Puthoff, Fundamentals of Quantum Electronics, (Wiley, New York, 1969), pp. 65–70.

3. R.A. McClatchey, W.S. Benedict, S.A. Clough, D.E. Burch, R.F. Calfee, K. Fox, L.S. Rothman and J.S. Garing, AFCRL atmospheric absorption line parameters compilation, AFCRL-TR-0096 (1973).

4. L.S. Rothman, S.A. Clough, R.A. McClatchey, L.G. Young, D.E. Snider and A. Goldman, AFGL trace gas compilation, Appl. Opt., 17, 507 (1978).

5. L.S. Rothman, Update of the AFGL atmospheric absorption line parameters compilation, Appl. Opt., 17, 3517 (1978).

6. L.S. Rothman, AFGL atmospheric absorption line parameters compilation: 1980 version, Appl. Opt., 20, 791 (1981).

7. L.S. Rothman, A. Goldman, J.R. Gillis, R.H. Tipping, L.R. Brown, J.S. Margolis, A.G. Maki and L.D.G. Young, AFGL trace gas compilation: 1980 version, Appl. Opt., 20, 1323 (1981).

8. L.S. Rothman, A. Goldman, J.R. Gillis, R.R. Gamache, H.M. Pichett, R.L. Poynter, N. Husson and A. Chedin, AFGL trace gas compilation: 1982 version, Appl. Opt., 22, 1616 (1983).

9. L.S. Rothman, R.R. Gamache, A. Barbe, A. Goldman, J.R. Gillis, L.R. Brown, R.A. Toth, J.-M. Flaud and C. Camy-Peyret, AFGL atmospheric absorption line parameters calculation: 1982 edition, Appl. Opt., 22, 2247 (1983).

10. L.S. Rothman, R.R. Gamache, A. Goldman, L.R. Brown, R.A. Toth, H.M. Pickett, R.L. Pognter, J.M. Flaud, C. Camy-Peyret, A. Barbe, N. Husson, C.P. Rinsland and M.A.H. Smith, The HITRAN database: 1986 edition, Appl. Opt., 26, 4058 (1987).

11. J.E.A. Selby and R.A. McClatchey, Atmospheric transmittance from 0.25 to 28.5 μm: Computer code LOWTRAN2, AFCRL-TR-72-0745, AD763 721 (1972).

12. J.E.A. Selby and R.A. McClatchey, Atmospheric transmittance from 0.25 to 28.5 μm: Computer code LOWTRAN3, AFCRL-TR-75-0255, ADA017 734 (1975).

13. J.E.A. Selby, E.P. Shettle and R.A. McClatchey, Atmospheric transmittance from 0.25 to 28.5 μm: Supplement LOWTRAN3B, AFGL-TR-76-0258, ADA040 701 (1976).

14. J.E.A. Selby, F.X. Kneizys, J.H. Chetwynd and R.A. McClatchey, Atmospheric transmittance/radiance: Computer code LOWTRAN4, AFGL-TR-78-0053, ADA058 (1978).

15. F.X. Kneizys, E.P. Shettle, W.O. Gallery, J.H. Chetwynd, L.W. Abrew, J.E.A. Selby, R.W. Fenn and R.A. McClatchey, Atmospheric transmittance/radiance: Computer code LOWTRAN5, AFGL-TR-80-067 (1980).

16. F.X. Kneizys et al., Atmospheric transmittance/radiance: Computer code LOWTRAN6, AFGL-TR-83-0187 (1983).

17. R.R. Gruenzel, Mathematical expressions for molecular absorption in LOWTRAN 3B, Appl. Opt., 17, 2591 (1978).

18. J.H. Pierluissi, K. Tomiyama and R.B. Gomez, Analysis of the LOWTRAN transmission functions, Appl. Opt., 18, 1607 (1978).

19. W.M. Cornette, Suggested modification to the total volume molecular scattering coefficient in LOWTRAN, Appl. Opt., 19, A182 (1980).

20. E.P. Shettle, F.X. Kneizys and W.O. Gallery, Suggested modification to the total volume molecular scattering coefficient in LOWTRAN: Comment, Appl. Opt., 19, 2873 (1980).

21. D.C. Robertson, L.S. Bernstein, R. Haimes, J. Wunderlich and L. Vega, 5-cm^{-1} band model option to LOWTRAN5, Appl. Opt., 20, 3218 (1981).

22. J.H. Pierluissi and G. Peng, New molecular transmission band models for LOWTRAN, Opt. Eng., 24, 541 (1985).

23. J.H. Pierluissi and C.-M. Tsai, New LOWTRAN models for the uniformly mixed gases, Appl. Opt., 26, 616 (1987).

24. D.E. Novoseller, Use of LOWTRAN in transmission calculations, Appl. Opt., 26, 3185 (1987).

25. D.E. Burch, W. France and D. Williams, Total absorptance of water vapor in the near infrared, Appl. Opt., 2, 585 (1963).

26. J.N. Howard et al., Infrared transmission of synthetic atmospheres. III. Absorption by water vapor, J. Opt. Soc. Am., 46, 242 (1956).

27. N.G. Yaroslavskii and A.E. Stanevich, The long wavelength infrared spectrum of H2O vapor and the absorption spectrum of atmospheric air in the region 20-2500 μ (500-4 cm-1), Opt. and Spectros., 7, 380 (1959).

28. J.N. Howard et al., Infrared transmission of synthetic atmospheres. II. Absorption by carbon dioxide, J. Opt. Soc. Am., 46, 237 (1956).

29. D.E. Burch, D.A. Gryvnak and D. Williams, Total absorptance of carbon dioxide in the infrared, Appl. Opt., 1, 759 (1962).

30. D.K. Edwards et al., Absorption by infrared bands of carbon dioxide gas at elevated pressures and temperatures, J. Opt. Soc. Am., 50, 130 (1960).

31. H.S. Gutowsky and E.M. Petersen, The infrared spectrum and structure of ozone, J. Chem. Phys., 18, 564 (1950).

32. M.K. Wilson and R.A. Ogg, The infrared spectrum and structure of ozone, J. Chem. Phys., 18, 766 (1950).

33. D.J. McCaa and J.H. Shaw, The infrared spectrum of ozone, J. Molec. Spectrosc., 25, 374 (1968).

34. H.C. Allen and E.K. Plyler, ν_3 band of methane, J. Chem. Phys., 26, 972 (1957).

35. G.M. Hoover and D. Williams, Infrared absorptance of carbon monoxide at low temperatures, J. Opt. Soc. Am., 59, 28 (1969).

36. D.E. Burch and D. Williams, Total absorptance by nitrous oxide bands in the infrared, Appl. Opt., 1, 473 (1962).

37. S.L. Bragg and J.D. Kelley, Atmospheric water vapor absorption at 1.3 μm, Appl. Opt., 26, 506 (1987).

38. S.A. Lawton and S.L. Bragg, Photoacoustic absorption spectra of atmospheric gases near 7603 cm^{-1}, Appl. Opt., 23, 3042 (1984).

39. S.L. Bragg, S.A. Lawton and C.E. Wiswall, Absolute measurements of absorption at the iodine-laser frequency in atmospheric gases, Opt. Lett., 10, 321 (1985).

40. T.A. Wiggins, Water vapor absorption at the atomic iodine laser line, Appl. Opt., 20, 3481-3483 (1981).

41. V.E. Zuev, Development of lasers and spectral equipment for measurement of atmospheric molecular gases, Topical Meeting on Laser and Optical Remote Sensing: Instrumention and Techniques Technical Digest Series, 1987, Volume 18, (Opt. Soc. of Am., Washington, D.C., 1978) p. MBI-1.

42. H.A. Gebbie et al., Atmospheric transmission in the 1 to 14 μ region, Proc. R. Soc. London Ser. A, 206, 87 (1951).

43. J.H. Taylor and H.W. Yates, Atmospheric transmission in the infrared, J. Opt. Soc. Am., 47, 223 (1956).

44. J.L. Streete, J.H. Taylor and S.L. Ball, Near infrared atmospheric absorption over a 25-km horizontal path at sea level, Appl. Opt., 6, 489 (1967).

45. J.L. Streete, Infrared measurements of atmospheric transmission at sea level, Appl. Opt., 7, 1545 (1968).

46. K.M. Haught and J.A. Dowling, Long-path high-resolution field measurements of absolute transmission in the 3.5 to 4.0 μm atmospheric window, Opt. Lett., 1, 121 (1977).

47. A. Ben-Shalom, D. Cabib., A.D. Devir, D. Goldschmidt, S.G. Lipson and U.P. Oppenheim, Spectral characteristics of infrared transmittance of the atmosphere in the region 2.8-14 micron--preliminary results, Infrared--Phys., 20, 165 (1980).

48. D.R. Cutten, Atmospheric broadband transmission measurements and predictions in the 8-13 μm window: Influence of water continuum absorption errors. Appl. Opt., 24, 1085 (1985).

49. K.M. Haught and D.M. Cordray, Long-path high resolution atmospheric transmission measurements: Comparison with LOWTRAN3B predictions, Appl. Opt., 17, 2668 (1978).

50. A. Ben-Shalom, A.D. Devir, S.G. Lipson and U.P. Oppenheim, Long-path high resolution atmospheric transmission measurements: Comparison with LOWTRAN3B predictions: Comments, Appl. Opt., 20, 171 (1981).

51. D.R. Cutten, Atmospheric transmission measurements and predictions in the 2100–2300-cm^{-1} region: Comparison of LOWTRAN6 and FASCOD models, Appl. Opt., 25, 593 (1986).

52. D.M. Gates and W.J. Harrop, Infrared transmission of the atmosphere to solar radiation, Appl. Opt., 2, 887 (1963).

53. K.Y. Kondratyev et al., Balloon investigations of radiative fluxes in the free atmosphere, Pure Appl. Geophys., 58, 187 (1964).

54. K.Y. Kondratyev, S.D. Andreev, I. Ya. Badinov, V.S. Grishechkin and L.V. Popova, Atmospheric optics investigations on Mt. Elbrus, Appl. Opt., 4, 1069 (1965).

55. D.G. Murcray et al., Atmospheric absorptions in the infrared at high altitudes, J. Opt. Soc. Am., 50, 107 (1960).

56. D.G. Murcray et al., Comparison of experimental and theoretical slant path absorptions in the region from 1400 to 2500 cm^{-1}, J. Opt. Soc. Am., 55, 1239 (1965).

57. P. Koepke and H. Quenzel, Water vapor: Spectral transmission at wavelengths between 0.7 μm and 1 μm, Appl. Opt., 17, 2114 (1978).

58. R. Guzzi, C. Tomasi and O. Vittori, Evidence of particulate extinction in the near infrared spectrum of the sun, J. Atmos. Sci., 29, 517 (1972).

59. C. Tomasi, R. Guzzi and O. Vittori, A search for the effect in the atmospheric water vapor continuum, J. Atmos. Sci., 31, 255 (1974).

60. O. Vittori, C. Tomasi and R. Guzzi, Dessens' droplets in the near and middle infrared spectrum of the sun, J. Atmos. Sci., 31, 261 (1974).

61. R.E. Bird, R.L. Hulstrom, A.W. Kliman and H.G. Eldering, Solar spectral measurements in the terrestrial environment, Appl. Opt., 21, 1430 (1982).

62. R. Guzzi and R. Rizzi, Water vapor absorption in the visible and near infrared: Results of field measurements, Appl. Opt., 23, 1853–1861 (1984).

63. V.E. Cachorro, A.M. de Frutos and J.L. Casanova, Medida de la irradiancia solar espectral en ei rango 400–1000 nm: Su evolusion con diversos parametras atmosfericas, Opt. Pur. Apl., 18, 135 (1985).

64. V.E. Cachorro, A.M. de Frutos and J.L. Casanova, Comparison between various models of solar spectral irradiance and experimental data, Appl. Opt., 24, 3249 (1985).

65. V.E. Cachorro, A.M. de Frutos and J.L. Casanova, Absorption by oxygen and water vapor in the real atmosphere, Appl. Opt., 26, 501 (1987).

66. D. Spitzer and M.R. Wernand, Assessment of solar irradiance spectra, Appl. Opt., 25, 2466 (1986).

67. G.H. Suits, Natural sources, The Infrared Handbook, W.L. Wolfe and G.Y. Zissis, eds. (Environmental Research Institute of Michigan, Ann Arbor, 1978), pp. 3-34.

68. E.J. McCartney, Optics of the Atmosphere (Wiley, New York, 1976).

69. L. Elterman, UV, visible and IR attenuation for altitudes to 50 km, 1968, AFCRL-TR-68-0153 (1968).

70. L. Elterman, Vertical attenuation model with eight surface- meteorological ranges 2 to 13 km, AFCRL-TR-70-0200 (1970).

71. G. Mie, A contribution to the optics of turbid media, especially colloidal metallic suspensions, Ann. Phys., 25, 377 (1908).

72. H. Holl, Optik, 4, 173 (1948).

73. A.N. Lowan, Tables of scattering functions for spherical particles, Appl. Math. Series 4, National Bureau of Standards (1949).

74. H.G. Houghton and W.R. Chalker, Scattering cross-sections of water drops in air for visible light, J. Opt. Soc. Am., 39, 955 (1949).

75. R.O. Gumprecht and C.M. Sliepcevich, Tables of Scattering Functions for Spherical Particles, (University of Michigan Press, Ann Arbor, 1951).

76. W.J. Pangonis et al., Tables of Light Scattering Functions of Spherical Particles, (Wayne State University Press, Detroit, 1957).

77. J.B. Havard, On the radiational characteristics of water clouds at infrared wavelengths, Ph.D. thesis, University of Washington, Seattle (1960).

78. D. Deirmendjian, Tables of Mie scattering cross sections and amplitudes, R-407-PR, Rand Corporation, Santa Monica (1963).

79. R. Penndorf, New tables of total Mie scattering coefficients for spherical particles of real refractive index ($1.33 \leq n \leq 1.50$), J. Opt. Soc. Am., 47, 1010 (1957).

80. W.M. Irvine and J.B. Pollack, Infrared optical properties of water and ice spheres, Icarus, 8, 324 (1968).

81. J.L. Zelmanovich and K.S. Shifrin, Tables of Light Scattering. Part III: Coefficients of Extinction, Scattering, and Light Pressure, (Hydrometeorological Publishing House, Leningrad, 1968).

82. D. Deirmendjian, Scattering and polarization properties of polydispersed suspensions with partial absorption, in Electromagnetic Scattering, M. Kerker, ed. (Macmillan, New York, 1963).

83. D. Deirmendjian, Scattering and polarization properties of water clouds and hazes in the visible and near infrared, Appl. Opt., 3, 187 (1964).

84. D. Deirmendjian, Electromagnetic Scattering on Spherical Polydispersions (Elsevier, New York, 1969.)

85. C.E. Junge, Atmospheric chemistry, in Advances in Geophysics, Vol 4 (Academic Press, New York, 1958).

86. C.E. Junge, Aerosols in Handbook of Geophysics, C.F. Campen et al., eds, (Macmillan, New York, 1960).

87. C.E. Junge, Air Chemistry and Radioactivity, (Academic Press, New York, 1963).

88. R.E. Pasceri and S.K. Friedlander, Measurements of the particle size distribution of the atmospheric aerosol. II. Experimental results and discussion, J. Atmos. Sci., 22, 577 (1965).

89. W.E. Clark and K.T. Whitby, Concentration and size distribution measurements of atmospheric aerosols and a test of the theory of self-preserving size distributions, J. Atmos. Sci., 24, 677 (1967).

90. R.F. Pueschel and Noll, Visibility and aerosol size frequency distribution, J. Appl. Meteorol., 6, 1045 (1967).

91. I.H. Blifford, Jr. and L.D. Ringer, The size and number distribution of aerosols in the continental troposphere, J. Atmos. Sci., 26, 716 (1969).

92. K.T. Whitby et al., The Minnesota aerosol analyzing system used in the Los Angeles smog project, J. Colloid Interface Sci., 39, 136 (1972).

93. K.T. Whitby et al., The aerosol size distribution of Los Angeles smog, J. Colloid Interface Sci., 39, 177 (1972).

94. I.H. Blifford, Jr., Tropospheric aerosols, J. Geophys. Res., 75, 3099 (1970).

95. D.A. Gillette and I.H. Blifford, Jr., Composition of tropospheric aerosols as a function of altitude, J. Atmos. Sci., 28, 1197 (1971).

96. D.J. Hoffman et al., Stratospheric aerosol measurements. I. Time variations at northern midlatitudes, J. Atmos. Sci., 32, 1446 (1975).

97. J.M. Rosen Simultaneous dust and ozone soundings over North and Central America, J. Geophys. Res., 73, 479 (1968).

98. J.M. Rosen et al., Stratospheric aerosol measurements. II. The worldwide distribution, J. Atmos. Sci., 32, 1457 (1975).

99. R.G. Pinnick et al., Stratospheric aerosol measurements. III. Optical model calculations, J. Atmos. Sci., 33, 304 (1976).

100. E.O. Hulbert, Observations of a searchlight beam to an altitude of 28 kilometers, J. Opt. Soc. Am., 27, 377 (1937).

101. E.O. Hulbert, Optics of searchlight illumination, J. Opt. Soc. Am., 36, 483 (1946).

102. E.A. Johnson et al., The measurement of light scattered by the upper atmosphere from a search-light beam, J. Opt. Soc. Am., 29, 512 (1939).

103. I.I. Romantzov and I.A. Khvostikov, Tropopause photography in polarized light, Compt. Rend. Acad. Sci., U.S.S.R., 53, 703 (1946).

104. L. Elterman, Aerosol measurements in the troposphere and stratosphere, Appl. Opt., 5, 1769 (1966).

105. G.G. Goyer and R.D. Watson, Laser techniques for observing the upper atmosphere, Bull. Am. Meteorol. Soc., 49, 890 (1968).

106. R.T. Collis, Lidar, Appl. Opt., 9, 1782 (1970).

107. W.E. Evans and R.T. Collis, Meteorological applications of lidar, Soc. Photogr. Inst. Eng., 8, 38 (1970).

108. G.B. Northlam et al., Dustsonde and lidar measurements of stratospheric aerosols: A comparison, Appl. Opt., 13, 2416 (1974).

109. A. Cohen and M. Graber, Laser-radar polarization measurements of the lower stratospheric aerosol layer over Jerusalem, J. Appl. Meteorol., 14, 400 (1975).

110. M.J. Post, F.F. Hall, R.A. Richter and T.R. Lawrence, Aerosol backscattering profiles at λ = 10.6 μm, Appl. Opt., 21, 2442 (1982).

111. M.J. Post, Aerosol backscattering profiles at CO_2 wavelengths: The NOAA data base, Appl. Opt., 23, 2507 (1984).

112. G.A. Newkirk, Jr., Photometry of the solar aureole, J. Opt. Soc. Am., 46, 1028 (1956).

113. G.A. Newkirk, Jr. and J.A. Eddy, Light scattering by particles in the upper atmosphere, J. Atmos. Sci., 21, 35 (1964).

114. A.E. Green et al., Interpretation of the sun's aureole based on atmospheric aerosol models, Appl. Opt., 10, 1263 (1971).

115. A.E. Green et al., Light scattering and the size-altitude distribution of atmospheric aerosols, J. Colloid Interface Sci., 39, 520 (1972).

116. G. Ward et al., Atmospheric aerosol index of refraction and size-altitude distribution from bi-static laser scattering and solar aureole measurements, Appl. Opt., 12, 2585 (1973).

117. D. Deirmendjian, A survey of light scattering techniques used in the remote monitoring of atmospheric aerosols, Rev. Geophys. Space Phys., 18, 341, (1980).

118. T. Nakajima, M. Tanaka and T. Yamaguchi, Retrieval of the optical properties of aerosols from aureole and extinction data, Appl. Opt., 22, 1951 (1983).

119. N.T. O'Neill and J.R. Miller, Combined solar aureole and solar beam extinction measurements, Parts 1 and 2, Appl. Opt., 23, 3691 (1984).

120. J.A. Curcio and K.A. Durbin, Atmospheric transmission in the visible, NRL Rept. 5368 (1959).

121. H.W. Yates and J.H. Taylor, Infrared transmission of the atmosphere, NRL Rept. 5453 (1960).

122. J.A. Curcio et al., Atmospheric scattering in the visible and infrared, NRL Rept. 5567 (1961).

123. J.A. Curcio, Evaluation of atmospheric particle size from scattering measurements in the visible and infrared, J. Opt. Soc. Am., 51, 548 (1961).

124. Electro-optics Handbook, (Burle Industries Inc., 1968), p. 7.

125. L. Elterman, An atlas of aerosol attenuation and extinction profiles for the troposphere and stratosphere, AFCRL-66-828 (1966).

126. Technical Panel STP6-Space Communications, The Application of Optical Space Communications to Military Users Requirements (a users guide), (The Technical Cooperation Program, Australia, 1984) pp. 2-27.

127. S.G. Jennings, Backscatter and extinction measurements in cloud and drizzle at CO_2 wavelengths, Appl. Opt., 25, 2499 (1986).

128. R.G. Pinnick, S.G. Jennings, P. Chylek, C. Ham and W.T. Grandy, Jr., Backscatter and extinction in water clouds, J. Geophys. Res., 88, 6787 (1983).

129. R.H. Dubinsky, A.I. Carswell and S.R. Pal, Determination of cloud microphysical properties by laser backscattering and extinction measurements, Appl. Opt., 24, 1614 (1985).

130. R.G. Pinnick, S.G. Jennings, P. Chylek and H.J. Auvermann, Verification of a linear relationship between IR extinction, absorption, and liquid water content of fog, J. Atmos. Sci., 36, 1577 (1979).

131. R.G. Pinnick, S.G. Jennings and P. Chylek, Relationship between extinction, absorption, backscattering and mass content of sulfuric acid aerosols, J. Geophys. Res., 85, 4059 (1980).

132. G.C. Mooradian, M. Geller, L.B. Stotts, D.H. Stephens and R.A. Krautwald, Blue-green pulsed propagation through fog, Appl. Opt., 18, 429 (1979).

133. J.A. Curcio and G.L. Knestrick, Correlation of atmospheric transmission with backscattering, J. Opt. Soc. Am., 58, 686 (1968).

134. H. Vogt, Visibility measurement using backscattered light, J. Atmos. Sci., 25, 912 (1968).

135. W.H. Paik, M. Tebyani, D.J. Epstein, R.S. Kennedy and J.H. Shapiro, Propagation experiments in low-visibility atmospheres, Appl. Opt., 17, 899 (1978).

136. G.C. Mooradian and M. Geller, Temporal and angular spreading of blue- green pulses in clouds, Appl. Opt., 21, 1572 (1982).

137. E.A. Bucher and R.M. Lerner, Experiments on light pulse communication and propagation through atmospheric clouds, Appl. Opt., 12, 2401 (1973).

138. L. Schlessinger, R.F. Lutomirski and S.F. Feyimura, Analysis of Kauai downlink laser cloud propagation experiment, Pacific-Sierra Research Report 1119 (1981).

139. Surface Airways Observations, National Climatic Data Center, Federal Building, Asheville, NC, 28801.

140. R.S. Lawrence, G.R. Ochs and S.F. Clifford, J. Opt. Soc. Am., 60, 826 (1970).

141. L.R. Tsvang, Radio Sci., 4, 1175 (1969).

142. J.L. Bufton, P.O. Minott, M.W. Fitzmaurice and P.J. Titterton, J. Opt. Soc. Am., 62, 1068 (1972).

143. P.H. Pasricha, M. Mohan, D.K. Tiwari and B.M. Reddy, Height distribution of refractivity structure constant from radiosonde observations, Indian J. Radio Space Phys., 12, 12 (1983).

44. G.W. Gilman, H.B. Coxhead and F.H. Willis, Reflection of sound signals in the troposphere, J. Acoust. Soc. Am., 18, 274–283 (1946).

45. L.G. McAllister, Acoustic sounding of the lower troposphere, J. Atmos. Terr. Phys., 30, 1439–1440 (1968).

46. C.G. Little, Acoustic methods for the remote probing of the lower atmosphere, Proc. IEEE, 57, 571–578 (1969).

47. L.G. McAllister, J.R. Pollard, A.R. Mahoney and P.J.R. Shaw, Acoustic sounding--a new approach to the study of atmospheric structure, Proc. IEEE, 57, 579–587 (1969).

48. D.W. Beran, W.H. Hooke and S.F. Clifford, Acoustic echo-sounding techniques and their application to gravity-wave, turbulence and stability studies, Boundary Layer Meteorol., 4, 133–153 (1973).

49. M. Fukushima, Kin-ichiro Akita and H. Tanaka, Night-time profiles of temperature fluctuations deduced from two-year sodar observations, J. Meteorol. Soc. Jap., 53, 487–491 (1975).

50. D.N. Asimakopoulis, R.S. Cole, S.J. Caughey and B.A. Crease, A quantitative comparison between acoustic sounder returns and the direct measurement of atmospheric temperature fluctuations, Boundary Layer Meteorol., 10, 137–147 (1976).

51. E.H. Brown and F.F. Hall, Jr., Advances in atmospheric acoustics, Rev. Geophys. Space Phys., 16, 47–110 (1978).

52. E.E. Gossard, J.E. Gaynor, R.J. Zamora and W.D. Neff, Finestructure of elevated stable layers observed by sounder and in situ tower sensors, J. Atm. Sci., 42, 2156–2169 (1985).

53. D. Atlas, K.R. Hardy, K.M. Glover, I. Katz and T.G. Konrad, Tropopause detected by radar, Science, 153 1110–1112 (1966).

54. J.A. Lane, Radar echoes from tropospheric layers by incoherent backscatter, Electron. Lett., 3, 173–174 (1967).

55. K.R. Hardy and I. Katz, Probing the clear atmosphere with high power, high resolution radars, Proc. IEEE, 57, 468–480 (1969).

56. R.A. Kropfli, I. Katz, T.G. Konrad and E.B. Dobson, Simultaneous radar reflectivity measurements and refractive index spectra in the clear atmosphere, Radio Sci., 3, 991–994 (1968).

57. T.E. VanZandt, J.L. Green, K.S. Gage and W.L. Clark, Vertical profiles of refractivity turbulence structure constant: Comparison of observations by the Sunset Radar with a new theoretical model, Radio Sci., 13, 819–829 (1978).

58. K.S. Gage and B.B. Balsley, Doppler radar probing of the clear atmosphere, Bull. Amer. Meteorol. Soc., 59, 1074–1093 (1978).

59. R.B. Chadwick and K.P. Moran, Long-term measurements of C_n^2 in the boundary layer, Radio Sci., 15, 355–361 (1980).

60. B. Balsley and V.L. Peterson, Doppler-radar measurements of clear air turbulence at 1290 MHz, J. Appl. Meteorol., 20, 266–274 (1981).

161. E.E. Gossard, R.B. Chadwick, T.R. Detman and J. Gaynor, Capability of surface-based clear-air Doppler radar for monitoring meteorological structure of elevated layers, J. Climate Appl. Meteorol., 23, 474-485 (1984).

162. E.E. Gossard and R.G. Strauch, Radar Observations of Clear Air and Clouds (Elsevier, Amsterdam, 1983).

163. W.M. Protheroe, The motion and structure of stellar shadow-band patterns, Q.J.R. Meteorol. Soc., 90, 27-42 (1964).

164. A.A. Townsend, The interpretation of stellar shadow-bands as a consequence of turbulent mixing, Q.J.R. Meteorol. Soc., 91, 1-9 (1965).

165. A. Peskoff, Theory of remote sensing of clear-air turbulence profiles, J. Opt. Soc. Am., 58, 1032-1040 (1968).

166. D.L. Fried, Remote probing of the optical strength of atmospheric turbulence and of wind velocity, Proc. IEEE, 57, 415-420 (1969).

167. J.W. Strohbehn, Remote sensing of clear-air turbulence, J. Opt. Soc. Am., 60, 948-950 (1970).

168. Liang-chi Shen, Remote probing of atmosphere and wind velocity by millimeter waves, IEEE Trans. Antennas. Propag., AP-18, 493-497 (1970).

169. J. Vernin and F. Roddier, Experimental determination of two-dimensional spatiotemporal power spectra of stellar light scintillation. Evidence for a multi-layer structure of the air turbulence in the upper troposphere, J. Opt. Soc. Am., 63, 270-273 (1973).

170. G.R. Ochs, Ting-i Wang, R.S. Lawrence and S.F. Clifford, Refractive turbulence profiles measured by one-dimensional spatial filtering of scintillations, Appl. Opt., 15, 2504-2510 (1976).

171. R.E. Good, B.J. Watkins, A.F. Quesada, J.H. Brown and G.B. Loriot, Radar and optical measurements of C_n^2, Appl. Opt., 21, 3373-3376 (1982).

172. R.W. Lee, Remote probing using spatially filtered apertures, J. Opt. Soc. Am., 64, 1295-1303 (1974).

173. S.F. Clifford and J.H. Churnside, Refractive turbulence profiling using synthetic aperture spatial filtering of scintillation, Appl. Opt., 26, 1295-1303 (1987).

174. A. Rocca, F. Roddier and J. Vernin, Detection of atmospheric turbulent layers by spatiotemporal and spatioangular correlation measurements of stellar-light scintillation, J. Opt. Soc. Am., 64, 1000-1004 (1974).

175. Ting-i Wang, S.F. Clifford and G.R. Ochs, Wind and refractive-turbulence sensing using crossed laser beams, Appl. Opt., 13, 2602-2608 (1974).

176. S.F. Clifford, The classical theory of wave propagation in a turbulent medium, in Laser Beam Propagation in the Atmosphere, edited by J.W. Strohbehn (Springer-Verlag, New York, 1978) p. 24.

177. J.W. Strohbehn, Line-of-sight wave propagation through the turbulent atmosphere, Proc. IEEE, 56, 1301 (1968).

78. A.A.M. Saleh, An investigation of laser wave depolarization due to atmospheric transmission, IEEE J. Quantum Electron., QE-3, 540 (1967).

79. R.B. Muchmore and A.D. Wheelan, Frequency correlation of line-of-sight signal scintillations, IEEE Trans. Antennas and Propagation, AP-11, 46 (1951).

80. E.N. Bramley, Correlation of signal fluctuations at two frequencies in propagation through an irregular medium, Proc. IEEE, 115, 1439 (1968).

81. E. Brookner, Limit imposed by atmospheric dispersion on the minimum laser pulse width that can be transmitted undistorted, Proc. IEEE, 57, 1234 (1969).

82. E. Brookner, Atmosphere propagation and communication model for laser wavelengths, IEEE Trans. Commun. Tech., COM-18, 396 (1970).

83. M.A. Ellison and H. Seddon, Some experiments on the scintillation of stars and planets, Roy. Astron. Soc., 112, 73 (19[illegible]

84. J.H. Shapiro, Imaging and optical communication through atmospheric turbulence, in Laser Beam Propagation in the Atmosphere, edited by J.W. Strohbehn (Springer Verlag, New York, 1978) p. 199.

85. H.T. Yura, Atmospheric turbulence induced laser beam spread, Appl. Opt., 10, 2771 (1971).

86. R.F. Lutomirski and H.T. Yura, Propagation of a finite optical beam in an inhomogeneous medium, Appl. Opt., 10, 1652 (1971).

87. H.T. Yura, Mutual coherence function of a finite cross section optical beam propagating in a turbulent medium, Appl. Opt., 11, 1399 (1972).

88. H.T. Yura, Short-term average optical-beam spread in a turbulent medium, J. Opt. Soc. Am., 63, 567 (1973).

89. D.L. Fried, Optical heterodyne detection of an atmospherically distorted signal wavefront, Proc. IEEE, 55, 57 (1967).

90. D.L. Fried, Optical resolution through a randomly inhomogeneous medium for very long and very short exposures, J. Opt. Soc. Am., 56, 1372 (1966).

91. D.L. Fried, Atmospheric modulation noise in an optical heterodyne receiver, IEEE J. Quantum Electron., QE-3, 213 (1967).

92. D.L. Fried and G.E. Mevers, Evaluation of r_o for propagation down through the atmosphere, Appl. Opt., 13, 2620 (1974).

93. D.L. Walters, Atmospheric modulation transfer function for desert and mountain locations: r_o measurements, J. Opt. Soc. Am., 71, 406 (1981).

94. M.E. Gracheva, A.S. Gurvich, S.S. Kashkarov and VI. V. Pokasov, Similarity relations and their experimental verification for strong intensity fluctuations of laser radiation, in Laser Beam Propagation in the Atmosphere, edited by J.W. Strohbehn (Springer-Verlag, New York, 1978) p. 117.

95. T. Wang and J.W. Strohbehn, Log-normal paradox in atmospheric scintillations, J. Opt. Soc. Am., 64, 583 (1974).

196. D.A. DeWolf, Are strong irradiance fluctuations log-normal or Rayleigh distributed? J. Opt. Soc. Am., 59, 1455 (1969).

197. D.A. DeWolf, Waves in turbulent air: A phenomenological approach, Proc. IEEE, 62, 1523 (1974.

198. G.C. Valley and D.L. Knepp, Application of joint Gaussian statistics to interplanetary scintillation, J. Geophys. Res., 81, 4723 (1976).

199. L.R. Bissonnette and P.L. Wizinowich, Probability distribution of turbulent irradiance in a saturation regime, Appl. Opt., 18, 1590 (1979).

200. L.R. Bissonnette, Propagation model of laser beams in turbulence, J. Opt. Soc. Am., 73, 262 (1983).

201. E.J. Fremouw, R.C. Livingston and D.A. Miller, On the statistics of scintillating signals, J. Atmos. Terr. Phys., 42, 717 (1980).

202. K. Furutsu, Review of the theory of the irradiance distribution in a turbulent medium with a particular emphasis on analytical methods, Radio Sci., 14, 287 (1979).

203. R. Dashen, Distribution of intensity in a multiply scattering medium, Opt. Lett., 9, 110 (1984).

204. G. Parry and P.N. Pusey, K distributions in atmospheric propagation of laser light, J. Opt. Soc. Am., 69, 796 (1979).

205. R.L. Phillips and L.C. Andrews, Universal statistical model for irradiance fluctuations in a turbulent medium, J. Opt. Soc. Am., 72, 864 (1982).

206. L.C. Andrews and R.L. Phillips, I-K distribution as a universal propagation model of laser beams in atmospheric turbulence, J. Opt. Soc. Am. A, 2, 160 (1985).

207. T. Wang and J.W. Strohbehn, Perturbed log-normal distribution of irradiance fluctuations, J. Opt. Soc. Am., 64, 994 (1974).

208. J.W. Strohbehn, T. Wang and J.P. Speck, On the probability distribution of line-of-sight fluctuations of optical signals, Radio Sci., 10, 59 (1975).

209. J.H. Churnside and R.J. Hill, Probability density of irradiance scintillations for strong path-integrated refractive turbulence, J. Opt. Soc. Am. A, 4, 727 (1987).

210. J.H. Churnside and S.F. Clifford, Log-normal Rician probability-density function of optical scintillations in the turbulent atmosphere, J. Opt. Soc. Am. A, 4, 1923 (1987).

211. R.S. Lawrence and J.W. Strohbehn, A survey of clear-air propagation effects relevant to optical communications, Proc. IEEE, 58, 1523 (1970).

212. S.F. Clifford, G.R. Ochs and R.S. Lawrence, Saturation of optical scintillation by strong turbulence, J. Opt. Soc. Am., 64, 148 (1974).

213. R.J. Hill and S.F. Clifford, Theory of saturation of optical scintillation by strong turbulence for arbitrary refractive-index spectra, J. Opt. Soc. Am., 71, 675 (1981).

214. R.J. Hill, Theory of saturation by strong turbulence: Plane-wave variance and covariance and spherical-wave covariance, J. Opt. Soc. Am., 72, 212 (1982).

215. H.T. Yura, Physical model for strong optical-amplitude fluctuations in a turbulent medium, J. Opt. Soc. Am., 64, 59 (1974).

216. J.W. Strohbehn, Modern theories in the propagation of optical waves in a turbulent medium, in Laser Beam Propagation in the Atmosphere, edited by J.W. Strohbehn (Springer-Verlag, New York, 1978), pp. 45-106.

217. M.E. Gracheva, A.S. Gurvich and M.A. Kallistratova, Measurements of the variance of 'strong' intensity fluctuations of laser radiation in the atmosphere, Izv. Vyssh. Ucheb. Zaved. Radiofiz., 13, 55 (1970).

218. D.L. Fried, Aperture averaging of scintillation, J. Opt. Soc. Am., 57, 169 (1967).

219. R.F. Lutomirski and H.T. Yura, Aperture averaging factor of a fluctuating light signal, J. Opt. Soc. Am., 59, 1247 (1969).

220. M.E. Gracheva and A.S. Gurvich, The averaging effect of the receiving aperture on light intensity fluctuations, Izv. Vyssh. Ucheb. Zaved. Radiofiz., 12, 253 (1969).

221. E.E. Bell, L. Eisner, J. Young and R.A. Oetjen, Spectral radiance of sky and terrain at wavelengths between 1 and 20 microns. II. Sky measurements, J. Opt. Soc. Am., 50, 1313 (1960).

222. Z. Sekera, Recent developments in the study of the polarization of skylight, in Advances in Geophysics, Volume 3 (Academic Press, New York, 1956).

223. S. Chandrasekhar and D.D. Elbert, The illumination and polarization of the sunlit sky on Rayleigh scattering, Trans. Am. Phil. Soc., 44, 643 (1954).

224. J.V. Dave and P.M. Furukawa, Scattered radiation in the ozone absorption bands at selected levels of a terrestrial, Rayleigh atmosphere, Meteorol. Monogr. 7, (1966).

225. D. Deirmendjian and Z. Sekera, Quantitative evaluation of multiply scattered and diffusely reflected light in the direction of a stellar source in a Rayleigh atmosphere, J. Opt. Soc. Am., 43, 1158 (1953).

226. J.V. Dave, Multiple scattering in a non-homogeneous Rayleigh atmosphere, J. Atmos. Sci., 22, 273 (1965).

227. J.V. Dave and P.M. Furukawa, Intensity and polarization of the radiation emerging from an optically thick Rayleigh atmosphere, J. Opt. Soc. Am., 56, 394 (1966).

228. R.T. Brinkman et al., Atmospheric scattering of the solar flux in the middle ultraviolet, Appl. Opt., 6, 373 (1967).

229. K.L. Coulson, Effect of surface reflection on the angular and spectral distribution of skylight, J. Atmos. Sci., 35, 759 (1968).

230. R.S. Fraser and W.H. Walker, Effect of specular reflection at the ground on light scattered from a Rayleigh atmosphere, J. Opt. Soc. Am., 58, 636 (1968).

231. M. Kano, Effect of a concentrated turbid layer on the polarization of skylight, J. Opt. Soc. Am., 58, 789 (1968).

232. G.N. Plass et al., Matrix operator theory of radiative transfer. I: Raleigh scattering. Appl. Opt., 12, 314 (1973).

233. W.G. Blattner et al., Monte Carlo studies of the sky radiation at twilight, Appl. Opt., 13, 534 (1974).

234. F.E. Volg, Volcanic turbidity, skylight scattering functions, sky polarization, and twilights in New England during 1983, Appl. Opt., 23, 2589 (1984).

235. K.L. Coulson, Characteristics of skylight at the zenith during twilight as indicators of atmospheric turbidity. 1: Degree of polarization, Appl. Opt., 19, 3469 (1980).

236. K.L. Coulson, Characteristics of skylight at the zenith during twilight as indicators of atmospheric turbidity. 2: Intensity and color ratio, Appl. Opt., 20, 1517 (1981).

237. K.L. Coulson, Effects of the El Chichon volcanic cloud in the stratosphere of the polarization of light from the sky, Appl. Opt., 22, 1036 (1983).

238. K.L. Coulson, Effects of the El Chichon volcanic cloud in the stratosphere on the intensity of light from the sky, Appl. Opt., 22, 2265 (1983).

239. R. Sloan et al., Infrared emission spectrum of the atmosphere, J. Opt. Soc. Am., 45, 455 (1955).

240. R. Sloan et al., Thermal radiation from the atmosphere, J. Opt. Soc. Am., 46, 543 (1956).

241. H.E. Bennett et al., Distribution of infrared radiance over a clear sky, J. Opt. Soc. Am., 50, 100 (1960).

242. A. Goldman, D.G. Murcray, F.J. Murcray, W.J. Williams and J.N. Brooks, Distribution of water vapor in the stratosphere as determined from balloon measurements of atmospheric emission spectra in the 24-29 μ region, Appl. Opt., 12, 1045 (1973).

243. R.E. Jennings and A.F. Moorwood, Atmospheric emission measurements with a balloon-borne Michelion interferometer, Appl. Opt., 10, 2311 (1971).

244. D.G. Murcary, J.N. Brooks, N.J. Sible and H.C. Westdal, Optical measurements from high altitude balloons, Appl. Opt., 1, 121 (1962).

245. A. Ben-Shalom, B. Barzilai, D. Cabib, A.D. Devir, S.G. Lipson and U.P. Oppenheim, Sky radiance at wavelengths between 7 and 14 μm: Measurement, calculation, and comparison with LOWTRAN-4 predictions, Appl. Opt., 19, 838 (1980).

246. H.G. Hughes, W.J. Schade and L.R. Hitney, Effects of aerosols on low- elevation infrared sky radiances, Appl. Opt., 25, 1536 (1986).

247. V.R. Noonkester, Near horizon IR radiance: Results of a model for the 8-12-μm band, Appl. Opt., 26, 203 (1987).

248. W.A. Hovis, D.K. Clark, F. Anderson, R.W. Austin, W.H. Wilson, E.T. Baker, D. Ball, H.R. Gordon, J.L. Mueller, S.Y. El-Sayed, B. Sturm, R.C. Wrigley and C.S. Yentsch, Science, 210, 60 (1980).

249. H.R. Gordon, Removal of atmospheric effects from satellite imagery of the oceans, Appl. Opt., 17, 1631 (1978).

250. H.R. Gordon and D.K. Clark, Boundary-Layer Meteorol., 18, 299 (1980).

251. H.R. Gordon, D.K. Clark, J.L. Mueller and W.A. Hovis, Science, 210, 63 (1980).

252. H.R. Gordon, Reduction of error introduced in the processing of coastal zone color scanner-type imagery resulting from sensor calibration and solar irradiance uncertainty, Appl. Opt., 20, 207 (1981).

253. K.B. Kidwell, NOAA Polar Orbiter Data (TIROS-N, NOAA-6, NOAA-7, and NOAA-8) Users Guide, (NOAA, National Environmental Satellite, Data, and Information Service, National Climatic Data Center, Satellite Data Services Division, Washington, D.C., 1984).

254. A. Schwalb, The TIROS-N/NOAA A-G satellite series, NOAA Tech. Memo. NESS 95, Washington, D.C. (1979).

255. M.J. Duggin, D. Piwinski, V. Whitehead and G. Ryland, Evaluation of NOAA-AVHRR data for crop assessment, Appl. Opt., 21, 1373 (1982).

256. M.J. Duggin and D. Piwinski, Recorded radiance indices for vegetation monitoring using NOAA AVHRR data: atmospheric and other effects in multitemporal data sets, Appl. Opt., 23, 2620 (1984).

257. R.J.P. Lyon, F.R. Honey and G.I. Ballew, Proc. IEEE, 63, 244 (1975).

258. J. Otterman and R.S. Fraser, Remote Sensing Environ., 5, 247 (1976).

259. J. Otterman, S. Ungar, Y. Kaufman and M. Podolak, Remote Sensing Environ., 9, 115 (1980).

260. A.J. Richardson, Relating Landsat digital count values to ground reflectance for optically thin atmospheric conditions, Appl. Opt., 21, 1457 (1982).

261. A.G. Bell, On the production and reproduction of sound by light, Proc. Amer. Assoc. Adv. Science, 29 (1880).

262. Forrest M. Mims III, Light-Beam Communications (Howard W. Sans and Co., Indianapolis, 1975).

263. Monte Ross, Laser Receivers (Wiley, N. [illegible] 66).

264. William Pratt, Laser Communication Systems (Wiley, New York, 1969).

265. R.M. Gagliardi and S. Karp, Optical Communications (Wiley, New York, 1976).

266. L.G. Kazovsky, Transmission of Information in the Optical Waveband (Wiley, New York, 1978).

267. M. King and S. Kainer, Some parameters of a laser-type beyond-the- horizon communication link, Proc. IEEE, 53, 137-141 (1965).

268. R.S. Kennedy, Communication through optical scattering channels: An introduction, Proc. IEEE, 58, 1651-1665 (1970).

269. J.G. Proakis and J.H. Miller, An adaptive receiver for digital signaling through channels with intersymbol interference, IEEE Trans. Inform. Theory, IT-15, 484-497 (1969).

270. D. Hirsch. A simple adaptive equalizer for efficient data transmission. IEEE Trans. Commun., COM-18, 5-11 (1970).

271. D.A. George, R.R. Bowen and J.R. Storey. An adaptive decision feedback equalizer. IEEE Trans. Commun., COM-19, 281-292 (1972).

272. S.D. Personick. Bell Sys. Tech. J., 52, 843 (1973).

273. J.C. Cartledge. IEEE Trans. Commun., COM-26, 1103 (1978).

274. D.G. Messerschmitt. IEEE Trans. Commun., COM-26, 1110 (1978).

275. J.H. Churnside. Optical communications through a dispersive medium: A performance bound for photocounting, Appl. Opt., 20, 573-578 (1981).

276. D.L. Fried and R.A. Schmeltzer, The effect of atmospheric scintillation on an optical data channel--laser radar and binary communications, Appl. Opt., 6, 1729 (1967).

277. G.R. Heidbreder and R.L. Mitchell, IEEE Trans. Aerosp. Electron. Sys., AES-3, 5 (1967).

278. R.S. Kennedy and E.V. Hoversten. On the atmosphere as an optical communication channel, IEEE Trans. Inform. Theory, IT-14, 716-725 (1968).

279. E.V. Hoversten, R.O. Harger and S.J. Holme, Communication theory for the turbulent atmosphere, Proc. IEEE, 58, 1626-1650 (1970).

280. J.H. Churnside and C.M. McIntyre, Heterodyne receivers for atmospheric optical communications, Appl. Opt., 19, 582-590 (1980).

281. W.N. Peters and R.J. Arguello, Fading and polarization noise of a PCM/PL system, IEEE J. Quantum Electron., QE-3, 532-539 (1967).

282. S. Solimeno, E. Corti and B. Nicoletti. Optical communication in a turbulent media. J. Opt. Soc. Am., 60, 1245-1251 (1970).

283. M.C. Teich and S. Rosenberg. Photocounting array receivers for optical communication through the lognormal atmospheric channel. 1: Optimum and suboptimum receiver structures, Appl. Opt., 12, 2616-2624 (1973).

284. S. Rosenberg and M.C. Teich, Photocounting array receivers for optical communication through the lognormal atmospheric channel. 2: Optimum and suboptimum receiver performance for binary signaling, Appl. Opt., 12, 2625-2635 (1973).

285. S. Rosenberg and M.C. Teich, Photocounting array receivers for optical communication through the lognormal atmospheric channel. 3: Error bound for M-ary equal-energy orthogonal signaling. IEEE Trans. Inform. Theory, IT-19, 807-809 (1973).

286. W.E. Webb and J.T. Marino, Jr., Threshold detection in an on-off binary communications channel with atmosphereic scintillation, Appl. Opt., 14, 1413-1417 (1975).

287. J.H. Churnside and M.C. McIntyre, Averaged threshold receiver for direct detection of optical communications through the lognormal atmospheric channel, Appl. Opt., 16, 2669-2676 (1977).

288. J.R. Roland and C.E. Whited, Air Force Space Laser Communications, Proc. SPIE, 150, 2–7 (1978).

289. M. Ross, P. Freedman, J. Abernathy, G. Matarsov, J. Wolf and J.D. Barry, Space optical communications with the Nd:YAG laser, Proc. IEEE, 66, 319–346 (1978).

290. A videotape of the experiment was made, with an introduction by Lt. Col. T. Samondi of the U.S. Air Force Space Division, Los Angeles, CA.

291. M. Ross, Proc. IEEE, 56, 196 (1968).

292. L.J. Rosenkrautz, J. Appl. Phys., 43, 4603 (1972).

293. G.I. Farmer and Y.C. Kiang, J. Appl. Phys., 45, 1356 (1974).

294. L.C. Conant and C.W. Reno, GaAs laser diode pumped Nd:YAG laser, Appl. Opt., 13, 2457–2458 (1974).

295. K. Kubodera and K. Otsuka, Diode–pumped miniature solid–state laser: Design considerations, Appl. Opt., 16, 2747 (1977).

296. D.L. Sipes, Highly efficient neodymium:yttrium aluminum garnet laser end pumped by a semiconductor laser array, Appl. Phys. Lett., 47, 74–76 (1985).

297. B. Furch, A. Hahne, R. Holme and H. Lutz, Optical satellite links for ESA's space missions, Proc. SPIE, 810, 134–140 (1987).

298. W. Reiland, W. Englisch and M. Endemann, Optical intersatellite communication links: State of CO_2 laser technology, Proc. SPIE, 616, 69 (1986).

299. W. Reiland and M. Wittig, CO_2 laser technology for space applications, Proc. SPIE, 810, 150–156 (1987).

300. R. Kern, U. Kugel and E. Hettlage, Control of a pointing, acquisition, and tracking subsystem for intersatellite laser links ISL, Proc. SPIE, 810, 202–210 (1987).

301. R. Flatscher, W.R. Leeb, A.L. Scholtz and H.K. Philipp, Mechanically cooled receiver front end for high data rate CO_2 laser communication, Proc. SPIE, 810, 223–230 (1987).

302. G. Hacker, System considerations for an optical intersatellite/interorbit link based on Nd:YAG–laser technology, Proc. SPIE, 810, 157–163 (1987).

303. J.L. Vanhove, B. Laurent and J.L. Perbos, System analysis of optical interorbit communications, Proc. SPIE, 810, 157–163 (1987).

304. M. Hohner and S. Manhart, Piezoelectric scanners, Proc. SPIE, 810, 211– 214 (1987).

305. J.C. Boatemy, Use of CCD arrays for optical link acquisition and tracking, Proc. SPIE, 810, 215–222 (1987).

306. R. Hahn, A. Spallicci and A. Hahne, Transceiver in–flight checkout system, Proc. SPIE, 810, 232–238 (1987).

307. A.F. Popescu, W.R. Leeb and A.L. Scholtz, Laboratory model of a bidirectional diode laser data link with acquisition and tracking capability, Proc. SPIE, 810, 239–244 (1987).

308. J.L. Perbos and B. Laurent, Laser diodes communications for the European data relay system, Proc. SPIE, 756, (1987).

309. Y. Furuhama, K. Yasukawa, K. Kashiki and Y. Hirata, Present status of optical ISL studies in Japan, Proc. SPIE, 810, 141–149 (1987).

310. S. Karp, Optical communications between underwater and above surface (satellite) terminals, IEEE Trans. Comm., COM-24, 66–81 (1976).

311. G.C. Mooradian, Atmospheric, space, and underwater optical communications for naval applications, Proc. SPIE, 150, 83–91 (1978).

312. J.R. Kerr et al., Atmospheric optical communications systems, Proc. IEEE, 58, 1691–1709 (1970).

313. J.H. Shapiro and R.C. Harney, Simple algorithms for calculating optical communication performance through turbulence, Proc. SPIE, 295, 41–54 (1981).

314. R.L. Fante, Electromagnetic beam propagation in turbulent media: an update, Proc. IEEE, 68, 1424–1443 (1980).

315. H.T. Yura and W.G. McKinley, Optical scintillation statistics for IR ground-to-space laser communication systems, Appl. Opt., 22, 3353–3358 (1983).

316. V.W.S. Chan, Coding for the turbulent atmospheric optical channel, IEEE Trans. Com., COM-30, (1982).

317. K.S. Shaik, A heuristic weather model for optical communications through the atmosphere, TDA progress report, Jet Propulsion Laboratory, to be published.

318. D.P. Wylie and W.P. Menzel, Cloud cover statistics using VAS, SPIE's OE-LASE '88 Symposium on Innovative Science and Technology, Los Angeles, CA, 10–15 January 1988.

319. P. Brandinger, Propagation requirements for 30/20 GHz systems design, Spring USRI Meeting, Washington, D.C., 1978.

320. R.S. Englebrecht, The effect of rain on satellite communications above 10 GHz, RCA Review, 40, p. 191 (1979).